

DEVELOPMENT AND TESTING OF A BIOFEEDBACK SYSTEM FOR
WHEELCHAIR PROPULSION ANALYSIS

By

Liyun Guo

Dissertation

Submitted to the Faculty of the
Graduate School of Vanderbilt University

In partial fulfillment of the requirements

For the degree of

DOCTOR OF PHILOSOPHY

in

MECHANICAL ENGINEERING

May, 2012

Nashville, Tennessee

Approved:

Professor Nilanjan Sarkar

Doctor Mark Richter

Professor Michael Goldfarb

Professor Robert J. Webster, III

Professor Paul H. King

ACKNOWLEDGEMENTS

I would first like to thank my advisor, Dr. Nilanjan Sarkar and Dr. Mark Richter, for their continuous support, excellent advice and constant encouragement during the time I have been a graduate student at Vanderbilt University. I also want to thank Max-Mobility for providing me this research project opportunity.

I am grateful for all of the support that I have received from my family. I have wonderful and supportive parents who have always encouraged me in pursuit of my goals. I am also extremely grateful for my wife as she has patiently supported and encouraged me during my time in graduate school. Without their support, none of this would have been possible.

I have had the pleasure to work with many outstanding students and workers in the past 5 years, including Yandong Gao, Yu Tian and Jiashu Sun of Mechanical Engineering at Vanderbilt University, present and past workers of Max-Mobility: Adam Karpinski, Russell Rodriguez, Maureen Ann Linden, Andy, Josh, Ben et al. Last, I would like to thank all wheelchair subjects that participated in this research.

To my beloved wife, Xing, infinitely supportive

TABLE OF CONTENTS

	Page
ACKNOWLEDGEMENTS.....	ii
Table of Contents	iii
LIST OF TABLES	vi
LIST OF FIGURES	viii
I INTRODUCTION	1
1.1 Background and motivation	1
1.2 Manual wheelchair propulsion measurement	2
1.3 Biofeedback.....	6
1.4 Needs analysis	9
II THE OPTIPUSH SYSTEM design and validation.....	11
2.1 OptiPush Wheel Components and Structure	11
2.1.1 Force Sensor.....	13
2.1.2 Angle Sensor.....	14
2.1.3 Bluetooth module.....	15
2.1.4 Printed Circuit Board	16
2.2 OptiPush Software.....	20
2.2.1 Bluetooth setting.....	21
2.2.2 Offset Removing.....	21
2.2.3 Variables	23
2.2.4 Biofeedback.....	27

2.3	System validation.....	28
2.3.1	Wheel angle validation	29
2.3.2	Speed validation.....	29
2.3.3	Force and Torque validation.....	31
2.4	Conclusion.....	37
III	TESTING THE OPTIPUSH BIOFEEDBACK SYSTEM	39
3.1	Methods.....	39
3.1.1	Participants.....	39
3.1.2	Data Collection	40
3.1.3	Single-Variable Biofeedback	41
3.1.4	Data Analysis.....	44
3.2	Results.....	44
3.2.1	Participants.....	44
3.2.2	Viability of Biofeedback	44
3.3	Discussion	46
3.4	Conclusions.....	49
IV	MULTIVARIABLE BIOFEEDBACK DESIGN & TESTING.....	50
4.1	Multivariable biofeedback design.....	51
4.2	Multivariable biofeedback testing.....	54
4.2.1	Subjects.....	54
4.2.2	Data Collection	55
4.2.3	Data Analysis.....	59
4.3	Results.....	62

4.3.1	Participants.....	62
4.3.2	Effects of Education and Multivariable Biofeedback.....	62
4.4	Discussion.....	64
4.5	Conclusion.....	67
V	CONCLUSION AND FUTURE DIRECTIONS.....	68
5.1	Project summary.....	68
5.2	System application.....	68
5.3	Future Directions.....	71
5.4	Conclusion.....	73
	Appendix A: MAIN VI FRONT PANEL.....	75
	Appendix B OPTIPUSH TESTING REPORT.....	77
	Appendix C TREADMILL VALIDATION.....	78
	REFERENCE LIST.....	84

LIST OF TABLES

Table	Page
Table 2.1	Power needed for all active electrical components 18
Table 2.1	Results of wheel diameter testing at a tire pressure of 110 psi 30
Table 2.2	Results of wheel diameter testing at a tire pressure 90 psi 31
Table 2.3	Results for testing F_x and F_y with a reference load of 23.28N 33
Table 2.4	Results for testing F_x and F_y with a reference load of 68.04N 33
Table 2.5	Results for testing F_x and F_y with a reference load of 109.99N 34
Table 2.6	Results for testing F_z 34
Table 2.7	Results for testing torque 34
Table 2.8	Results of dynamic testing 37
Table 3.1	Targets for biofeedback variables 42
Table 3.2	Normal propulsion variables 45
Table 3.3	Changes to the target variable during each biofeedback condition 46
Table 3.4	Coefficient of variation (CV) for each biofeedback variable 48
Table 3.5	Breakdown of force data from the 'Decrease Peak Force by 10%' and 'Maximize Smoothness' conditions 48
Table 4.1	Primary instructions/recommendations on how to improve handrim biomechanics 58
Table 4.2	All trial results for a subject 61
Table 4.3	Mean \pm SD Handrim Biomechanics During Normal Treadmill Propulsion 62
Table 4.4	Percent Changes in Outcome Variables Compared to Normal Trial 63
Table 4.5	Data for 3 example subjects 67

Table 5.1	Comparison of propulsion variables between overground and treadmill	69
Table 5.2	Users of OptiPush Biofeedback System	71

LIST OF FIGURES

Figure	Page
Figure 1.1 Schematic drawing of the instrumented wheel described by de Groot et al.[7].	2
Figure 1.2 The Mayo Clinic's instrumented wheel.....	3
Figure 1.3 The SmartWheel.	4
Figure 1.4 The wired version of MAX Mobility's propulsimeter.....	4
Figure 1.5 The wireless version of the MAX Mobility with (A) and without (B) attachment of the electrical components and handrim.	5
Figure 1.6 Screen showing the velocity and FEF feedback given to the subjects.....	7
Figure 1.7 Wheelchair dynamometer with feedback on velocity, power output, and FEF.	8
Figure 1.8 SmartWheel biofeedback interface.	9
Figure 2.1 Assembly of the OptiPush wheel showing (a) the instrumentation module; (b) the attachment of the handrim and triangle to the IM; (c) the attachment of the wheel to the IMand (d) the OptiPush wheel on the wheelchair.....	12
Figure 2.2 Applied force and torque vector on load cell.	13
Figure 2.3 Absolute magnetic shaft encoder.	15
Figure 2.4 The absolute output of the encoder.	15
Figure 2.5 Bluetooth module.	16
Figure 2.6 Circuit diagram for manipulating load cell output signal; where V_{sgn} and V_{ref} are the output voltages of the load cell from one channel. 16	16
Figure 2.7 Circuit diagram for 5V resource by using TL431.	18
Figure 2.8 Printed circuit board.	19

Figure 2.9	Assembled instrumentation module.	19
Figure 2.10	Flowchart of the OptiPush software	20
Figure 2.11	Offset data collection.	22
Figure 2.12	An example of offset data.	23
Figure 2.13	The push and coast phases of the stroke.	24
Figure 2.14	Braking torque.....	24
Figure 2.15	OptiPush Software interface.	28
Figure 2.16	Load applied to the handrim for testing (a) F_x , F_y and (b) T_z	32
Figure 2.17	Centrifugal force (F_C) and gravity (F_G) of the metal block applied to the handrim for dynamic testing; where θ is wheel angle and α is the angle of metal block.	35
Figure 2.18	Measured F_x and reference F_x at a treadmill speed 1.0m/s with 1.174 kg metal block attached to the handrim.....	36
Figure 2.19	Measured T_z and reference T_z at a treadmill speed of 1.0m/s with a 1.174 kg metal block attached to the handrim.....	36
Figure 3.1	The testing setup (a) and biofeedback display (b) used in this study.	43
Figure 4.1	Multivariable biofeedback interface	54
Figure 4.2	Education video that demonstrated (a) contact angle; (b) longer push stroke advantages.	57
Figure 4.3	Optipush biofeedback video that shows the target of multivariable biofeedback.....	58
Figure 4.4	Trends in percent changes in peak force versus percent changes in contact angle for each training component; where \circ = EDU and \bullet = BMB. The diamonds indicate the mean data point for each component.	64
Figure 5.1	Musculoskeletal model used in the wheelchair propulsion simulations.	70
Figure 5.2	The four classified stroke patterns	70
Figure 5.3	New strain gauge CAD design	72

Figure 5.4	The non-linearity near 0V and 5V output	73
Figure A-1	Interface of OptiPush software settings. (a) Bluetooth port selection; (b) Bluetooth connection; (c) Client information; (d) Wheel offset removal.	75
Figure A-2	Biofeedback interface of OptiPush software	76

CHAPTER I

INTRODUCTION

1.1 Background and motivation

Studies have shown that the manual wheelchair propulsion often results in pain and injury in the upper extremity (UE). In a study of 239 manual wheelchair users, Sie et al. found that 64% patients with paraplegia reported UE pain or injury, most commonly at the shoulder[1]. The presence of UE pain and injury can severely impact mobility, independence, and the quality of life. Wheelchair handrim propulsion technique has been found to be an important factor in explaining UE pain and injury[2-4]. Little is known about how wheelchair users push, how to optimally propel a wheelchair and how to change wheelchair user's propulsion pattern to the optimized propulsion. The main reason for the lack of information is the lack of comprehensive research tools for assessing and improving wheelchair propulsion. A new research tool as developed here, which can both measure wheelchair propulsion and provide critical feedback to users and clinicians, can be used to optimize propulsion technique and hopefully delay or prevent the development of the UE pain and injury.

1.2 Manual wheelchair propulsion measurement

As the study of manual wheelchair propulsion has progressed over the past 2 decades, so too have the tools used to measure handrim biomechanics. Van der Woude and colleagues began studying wheelchair propulsion using a stationary barber chair with test wheels attached[5] and later, in 1990, with a wheelchair ergometer[6]. In 2005, they built their own instrumented wheel[7]. A 3-dimensional (3D) force/torque transducer and potentiometer were installed between the right wheelchair wheel and hand rim (Figure 1.1). A bicycle speedometer with a digital display was attached to the left wheel of the chair to measure the propulsion velocity.

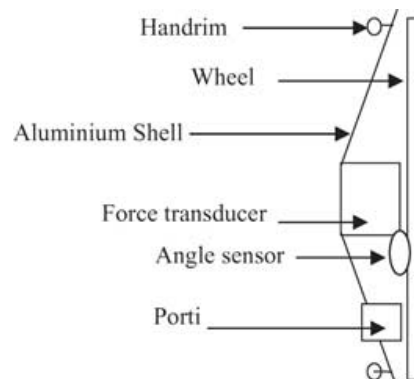


Figure 1.1 Schematic drawing of the instrumented wheel described by de Groot et al.[7].

Wu et al. at the Mayo Clinic have also built an instrumented wheel for studying wheelchair propulsion[8;9]. The instrumented wheel consists of a 6-component load cell, a handrim unit, a wheel and a data logger (Figure 1.2). The data logger was mounted to the wheel to record data from load cell and to transfer it to a personal computer after each trial. Five reflective markers for a

video-based motion system were placed on the face plate to determine the orientation and the position of the wheel.

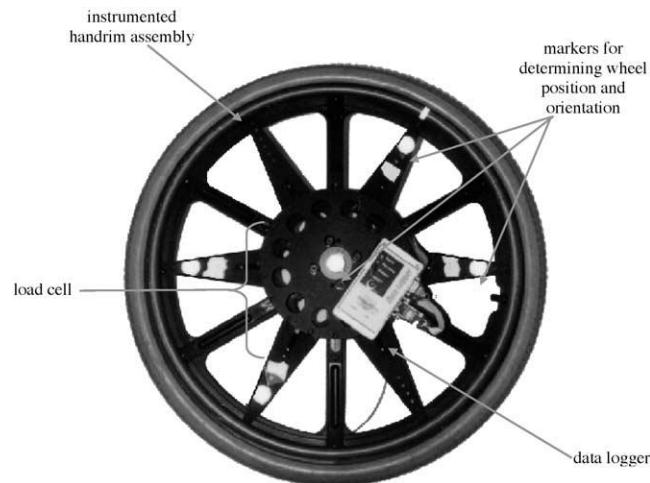


Figure 1.2 The Mayo Clinic's instrumented wheel.

Perhaps the most well-known and widely used instrumented wheelchair wheel, developed by Dr. Rory Cooper and his team at the University of Pittsburgh, is the SmartWheel[10;10-12]. The SmartWheel measures 3D forces and torques applied to the handrim using 3 instrumented beams, mounted 120° apart, which connect the handrim to the wheel. Each beam is fitted with two strain gauge bridges that detect deflection of the beam during handrim loading. An optical encoder is used to determine the position of the beams. All the signals are interfaced to an analog-to-digital board and then transferred wirelessly to a computer. In 2000, the SmartWheel was brought to market. (Figure 1.3) Since that time, the SmartWheel has been used by a number of researchers to study manual wheelchair propulsion[13-15].



Figure 1.3 The SmartWheel.

Another instrumented wheel (or propulsimeter), which would lay the foundation for the OptiPush Biofeedback system was developed by Dr. Mark Richter, President of MAX Mobility. The wheel was wired, yet the innovative external wiring configuration allowed the wheel to be used for treadmill propulsion testing (Figure 1.4).



Figure 1.4 The wired version of MAX Mobility's propulsimeter.

In 2004, the hardware on the propulsimeter was upgraded, including the addition of a wireless transmitter[16;17] and a 6-degree-of-freedom (DOF) load cell for measuring handrim loads. The load cell was mounted at the hub of the wheel and was attached to the handrim (Figure 1.5), so that loads applied to the

handrim were transferred to the wheel through the load cell. An absolute inclinometer was used to measure the wheel position (angle). Measurements from the load cell and the inclinometer were transferred to a data collection computer using a high-speed wireless LAN connection.



Figure 1.5 The wireless version of the MAX Mobility with (A) and without (B) attachment of the electrical components and handrim.

These propulsimeters are the major devices that have been used for wheelchair propulsion analysis. The SmartWheel is the most popular device since it is the only product on the market. The SmartWheel sells for around \$16,000 and is available in 22", 24", 25", and 26" wheel diameters; however, each additional size costs an extra \$5,000. The MAX Mobility propulsimeter can be fitted to different wheel sizes, but it was designed for post data processing and not for real-time biofeedback.

1.3 Biofeedback

Biofeedback is a process that enables an individual to learn how to change physiological activity for the purposes of improving health or performance. Precise instruments measure physiological activity such as brainwaves, heart function, breathing, muscle activity, and skin temperature. These instruments rapidly and accurately "feed-back" information to the user. The presentation of this information, often in conjunction with changes in thinking, emotions, and behavior, may support desired physiological changes. Over time, these changes can endure without continued use of an instrument[18]. Some researchers use propulsiometers and other devices to measure wheelchair user's propulsion and "feedback" information to the user.

Van der Woude et al. conducted a test with 20 able-bodied male subjects with no prior experience in wheelchair propulsion. Subjects were divided to two groups, an experimental group and a control group. Each practiced three weeks, three times per week, on a computer-controlled wheelchair ergometer[6]. The experimental group practiced with and the control group practiced without visual feedback on the fraction of effective force (FEF). This measure is defined as the ratio of effective (tangential) force to total force, expressed as a percentage, and was used to describe how effective an individual was at applying forces to the hand rim. Testing was conducted on a wheelchair ergometer that measures velocity and propulsion force. Feedback on FEF and velocity was presented on a screen in front of all subjects and feedback on FEF was shown only to the

experimental group (Figure 1.6). The results showed that the experimental group had a higher mean FEF than the control group[19].

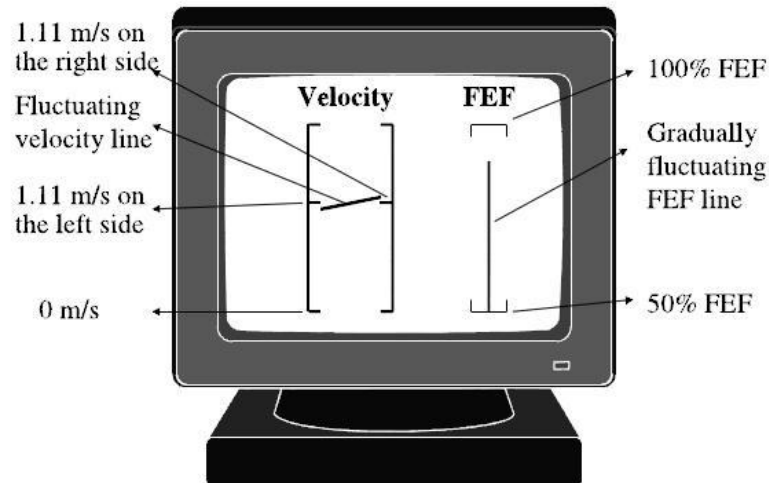


Figure 1.6 Screen showing the velocity and FEF feedback given to the subjects.

Kotajarvi et al. conducted a similar study to improve FEF with visual biofeedback[20]. The study included 18 experienced manual wheelchair users who propelled their own wheelchairs, equipped with a custom-built instrumented wheel (Figure. 1.2)[8;9], on a wheelchair dynamometer (Figure 1.7). The dynamometer provided a resistant force to the wheel. A monitor displaying visual biofeedback data was mounted in front of the subjects. The monitor provided immediate feedback on the FEF, velocity, and power output during the push phase of propulsion. All subjects propelled two trials: one with and one without feedback. In comparing the results, they found that the mean FEF did not change when experienced wheelchair users received real-time visual feedback.



Figure 1.7 Wheelchair dynamometer with feedback on velocity, power output, and FEF.

Degroot et al. did a test to examine the immediate and sustained effects of a verbal and visual training intervention on manual wheelchair users[21]. They tested 9 wheelchair users with the SmartWheel and the SmartWheel clinical software. The clinical software records and calculates several variables including push frequency, push length, peak push force, averaged push force and average speed (Figure 1.8). The variables are displayed on a laptop computer positioned in front of the participant. Subjects were asked to use long, smooth strokes and reduce push frequency as recommended by Boninger et al.[22] Results showed that push length increased and push frequency decreased with visual biofeedback. In general, visual biofeedback training can have a positive effect on the propulsion biomechanics.



Figure 1.8 SmartWheel biofeedback interface.

1.4 Needs analysis

MAX Mobility, LLC is a research and development company in Antioch, Tennessee dedicated to improving wheelchair technology and use. The Biomechanics Laboratory, which studies propulsion technique, relies on accurate measurement of handrim biomechanics. The wireless propulsimeter (Figure 1.5) used for data collection is functional and versatile (adaptable to 5 wheel sizes); however, it has several key limitations:

- 1) Wheel angle may be off by as much as 20 degrees.
- 2) The propulsimeter is heavy, weighing 14 pounds 5 ounces.
- 3) Wireless communication is unstable.
- 4) The system lacks biofeedback.

The objective of this project was to develop a wheelchair propulsion biofeedback system based on the MAX Mobility wireless propulsimeter. The system was required to: 1) measure dynamic propulsion forces and moments; 2) measure wheel angle without lag; 3) adapt to different sizes of wheels; 4) provide

stable wireless communication with a data collection computer; 5) provide real-time biofeedback of variables; and 6) save data for future processing.

CHAPTER II

THE OPTIPUSH SYSTEM DESIGN AND VALIDATION

A system was designed and fabricated to measure manual wheelchair propulsion, provide biofeedback and optimize propulsion technique. The system is named OptiPush Biofeedback System. The OptiPush Biofeedback System consists of two core components; the instrumented wheel, called the OptiPush Wheel, and the data collection, analysis, and biofeedback software called the OptiPush Software.

2.1 OptiPush Wheel Components and Structure

The OptiPush Wheel is composed of a handrim, a wheel, a triangular plate, three beams, three clamps and an Instrumentation Module (IM), which contains sensors and electrical components (Figure 2.1A). The clamps are attached to the ends of the triangular plate that is then mounted to the IM. Each beam is slid into one of the clamps and held secure with the clamp screw. The opposite ends of the beams are attached directly to the handrim using the preexisting tabs (Figure 2.1B). Different sized handrims can be attached by adjusting the length of the beams. Once the IM is fitted with the handrim, the wheel is attached to the IM by screwing the modified hub onto the three standoffs (Figure 2.1C). This design directs the loads applied to the handrim through the IM and then onto to the wheel. In addition, the simple assembly procedure allows the user to attach a

number of different wheels (and handrims), ranging in diameter from 20 inches (508 mm) to 26 inches (660 mm).

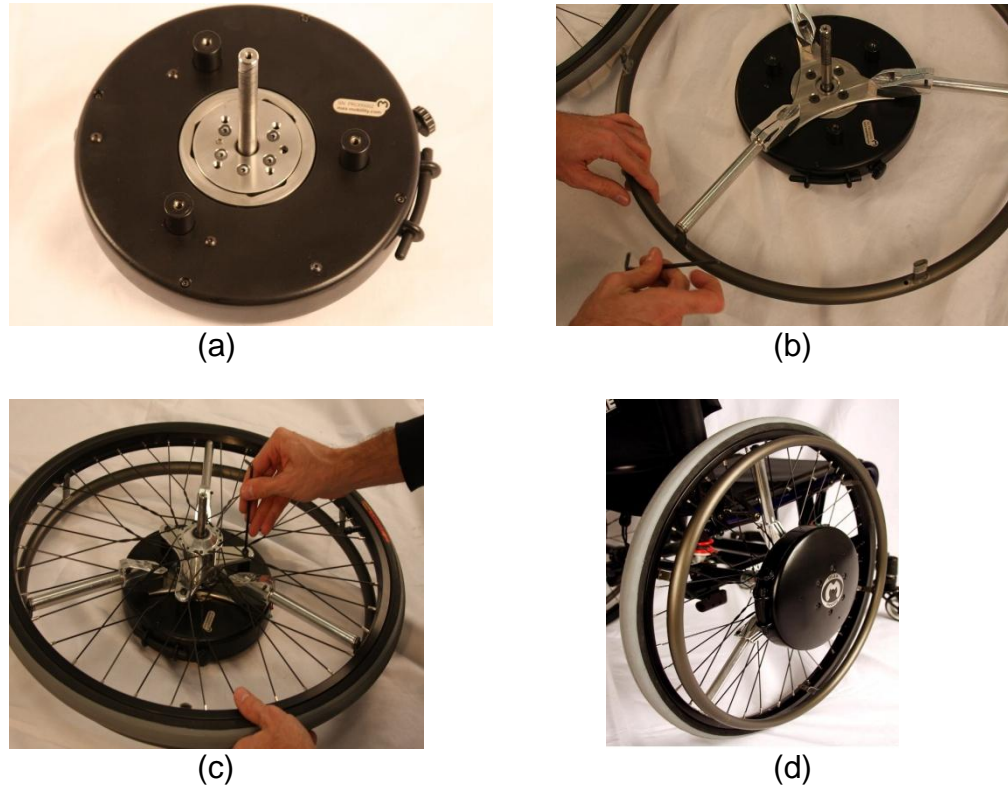


Figure 2.1 Assembly of the OptiPush wheel showing (a) the instrumentation module; (b) the attachment of the handrim and triangle to the IM; (c) the attachment of the wheel to the IM and (d) the OptiPush wheel on the wheelchair.

Once the OptiPush Wheel is assembled, it is attached to the wheelchair using a split-end axle that expands as the central screw is tightened. A matching wheel with a weighted disc, corresponding to the weight of the IM, is attached to the other side of the wheelchair to ensure symmetric wheel weights and inertias.

2.1.1 Force Sensor

The OptiPush Wheel measures three-dimensional forces and torques on the handrim using a commercially-available 6 degrees of freedom (DOF) load cell (Delta, ATI Industrial Automation, Apex, NC, USA). Figure 2.2 shows a drawing of the load cell and axes.

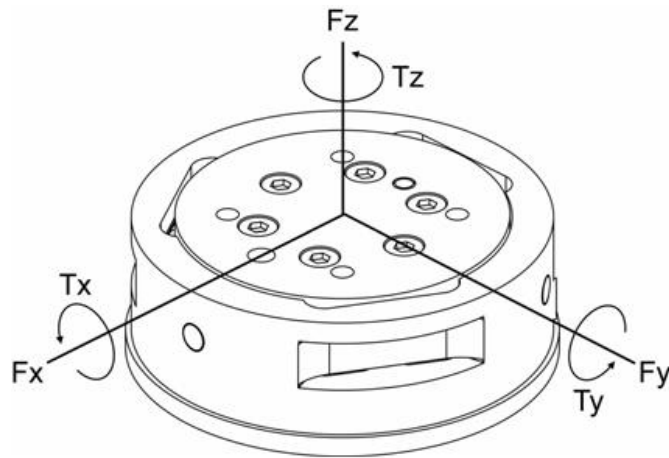


Figure 2.2 Applied force and torque vector on load cell.

The load cell is a monolithic structure that contains three beams, machined from a solid piece of metal, placed symmetrically inside. The force applied to the load cell flexes these three beams according to Hooke's law:

$$\sigma = E \cdot \varepsilon \quad (2.1)$$

Where σ is the stress applied to the beam (σ is proportional to force), E is the elasticity modulus of the beam and ε is the strain applied to the beam.

Semiconductor strain gauges are attached to the three beams and are considered strain-sensitive resistors. The resistance of the strain gauges change as a function of the applied strain as follows:

$$\Delta R = S_a \cdot R_o \cdot \varepsilon \quad (2.2)$$

Where ΔR is change in resistance of the strain gauge, S_a is the gauge factor of strain gauge, R_o is the resistance of strain gauge unstrained and ε is the strain applied to strain gauge.

The output voltages from the load cell are converted into forces and torques using a calibration matrix. The load cell had a full mechanical loading rate of 770N for F_x and F_y , 2310N for F_z and 70 Nm of moment for all directions. The max amount of error for all axes is 1.5% which is expressed as a percentage of its full-scale load. The load cell requires $\pm 15V$ for power and has an output range of $\pm 5V$. The resonant frequency of the load cell is 1500Hz for F_x , F_y , and T_z , and 1700Hz for T_x , T_y , and F_z . The load cell is mounted to the IM cover and attached to the load cell inner plate (Figure 2.1 B); therefore, loads applied to the handrim pass through the load cell and onto the wheel.

2.1.2 Angle Sensor

A rotary absolute magnetic shaft encoder (MA3, US Digital, Vancouver, WA, USA) is used to measure the wheel angle (Figure 2.3). The encoder reports the shaft position over 360° with no stops or gaps. It has 10-bit resolution and an analog voltage output of 0-5V that is proportional to absolute shaft position (Figure 2.4).



Figure 2.3 Absolute magnetic shaft encoder.

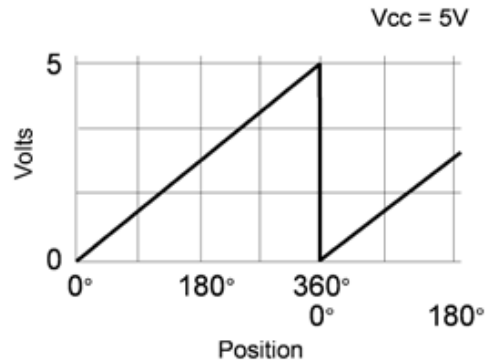


Figure 2.4 The absolute output of the encoder.

The encoder is mounted inside the IM. Since the IM is attached to the wheel by standoffs, the encoder rotates while the wheel rotates. A tooth gear is press fit to the encode shaft. The gear is linked (via a tooth belt) to a similar gear on the wheel axle such that when the wheel rotates, the shaft rotates the same amount relative to the encoder.

2.1.3 Bluetooth module

The IM captures and transfers data using a Bluetooth module (Blue Sentry RN-800S, Roving Networks Inc., Los Gatos, CA, USA). The module uses an 8 channel, 16 bit A/D converter to sample the 6 load cell signals and the encoder signal and convert them to a 0-5V, Bluetooth-enabled, digital data stream. Six channels are used to read load cell output while one channel is used to read the

encoder output. The last channel is used to measure a trigger channel which is used to synchronize with other devices. The module requires a 6-12VDC power supply and can transmit data up to 100 meters.



Figure 2.5 Bluetooth module.

2.1.4 Printed Circuit Board

A printed circuit board (PCB) is used to connect all electrical components such as resistors, capacitors, DC/DC converters, connectors and so on. The PCB provides power to all active electrical components and matches the sensor output ranges to the Bluetooth module input. Because the Bluetooth module can only sample analog signals from 0V to 5V, the output from the load cell ($\pm 5V$) is manipulated to 0-5V using a series of amplifiers shown in Figure 2.6.

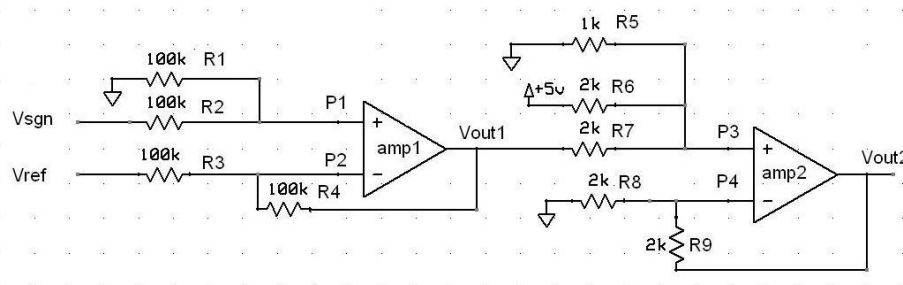


Figure 2.6 Circuit diagram for manipulating load cell output signal; where V_{sgn} and V_{ref} are the output voltages of the load cell from one channel.

From the diagram, the voltages at P1 and P2 are:

$$V_{P1} = V_{sgn} \cdot \frac{R_1}{R_1 + R_2} \quad (2.3)$$

$$V_{P2} = \frac{V_{ref} - V_{out1}}{R_3 + R_4} \cdot R_4 + V_{out1} \quad (2.4)$$

Since $V_{P1} = V_{P2}$ and $R_1 = R_2 = R_3 = R_4 = 100\text{K}\Omega$, Equations 2.3 and 2.4 can be expressed as:

$$V_{sgn} \cdot \frac{1}{2} = \frac{V_{ref} - V_{out1}}{2} + V_{out1}$$

$$V_{out1} = V_{sgn} - V_{ref} \quad (2.5)$$

The voltages at P3 and P4 are:

$$\frac{V_{out1} - V_{P3}}{R_7} + \frac{5V - V_{P3}}{R_6} = \frac{V_{P3}}{R_5}$$

$$V_{P3} = \frac{R_5 \cdot R_6 \cdot V_{out1} + 5V \cdot R_5 \cdot R_7}{R_5 \cdot R_6 + R_5 \cdot R_7 + R_6 \cdot R_7} \quad (2.6)$$

$$V_{P4} = V_{out} \cdot \frac{R_8}{R_8 + R_9} \quad (2.7)$$

Since $V_{P3} = V_{P4}$, $R_5 = 1\text{K}\Omega$, and $R_6 = R_7 = R_8 = R_9 = 2\text{K}\Omega$, Equations 2.6 and 2.7 can be reduced to:

$$\frac{V_{out1} + 5V}{4} = \frac{V_{out}}{2} \Rightarrow V_{out} = \frac{V_{out1} + 5V}{2} \quad (2.8)$$

From Equations 2.5 and 2.8 we calculated V_{out} as:

$$V_{out} = \frac{V_{sgn} - V_{ref} + 5V}{2} \quad (2.9)$$

The output range for the load cell is $\pm 5V$. By applying Equation 2.9, the range of V_{out} will be:

$$V_{out} = \frac{\pm 5V + 5V}{2} = \frac{0V \sim 10V}{2} = 0V \sim 5V \quad (3.0)$$

where V_{out} matches the input range of the Bluetooth module (0-5V). The voltage of power needed for all active electrical components are shown in Table 2.1.

Table 2.1 Power needed for all active electrical components

Components	Voltage (V)	Current (mA)
Load cell	±15 VDC	40
Bluetooth module	6-12VDC	60
Amplifiers	±12-15 VDC	1.4
Absolute encoder	4.5-5.5V	20

A ±12V (BWR-12/105-D5-C) converter and a ±15V (BWR-15/85-D5-C) converter is used to provide a clean and stable power supply to the load cell. A voltage reference chip TL431 is used to generate a stable 5V resource (Figure 2.7).

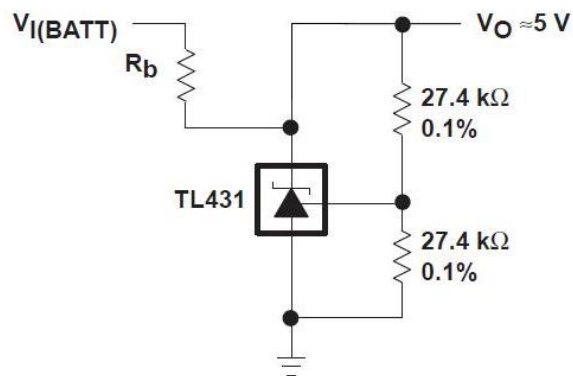


Figure 2.7 Circuit diagram for 5V resource by using TL431.

All components are powered by a 7.4V 2600mAh Li-ion battery. It can be used for more than three hours before recharging. The PCB also has some connectors to connect the battery, sensors and Bluetooth module.

The PCB was manufactured by ExpressPCB, which offers freeware to help design and draw the board. The finale design of the printed circuit board can be seen in Figure 2.8. The PCB, battery, encoder, Bluetooth module and load cell are secured inside the instrumentation module housing. The fully assembled IM can be seen in Figure 2.9.

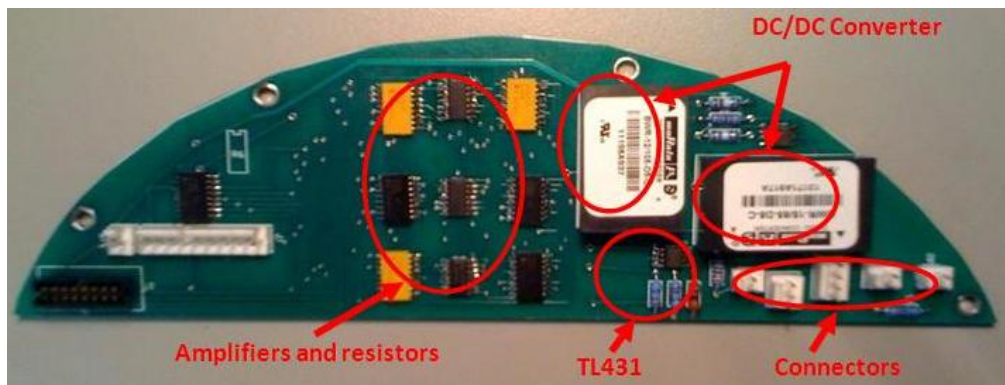


Figure 2.8 Printed circuit board.



Figure 2.9 Assembled instrumentation module.

2.2 OptiPush Software

The OptiPush Software was developed using LabVIEW (National Instruments Corporation, Austin, TX). A flowchart of the OptiPush Software was showed in figure 2.10.

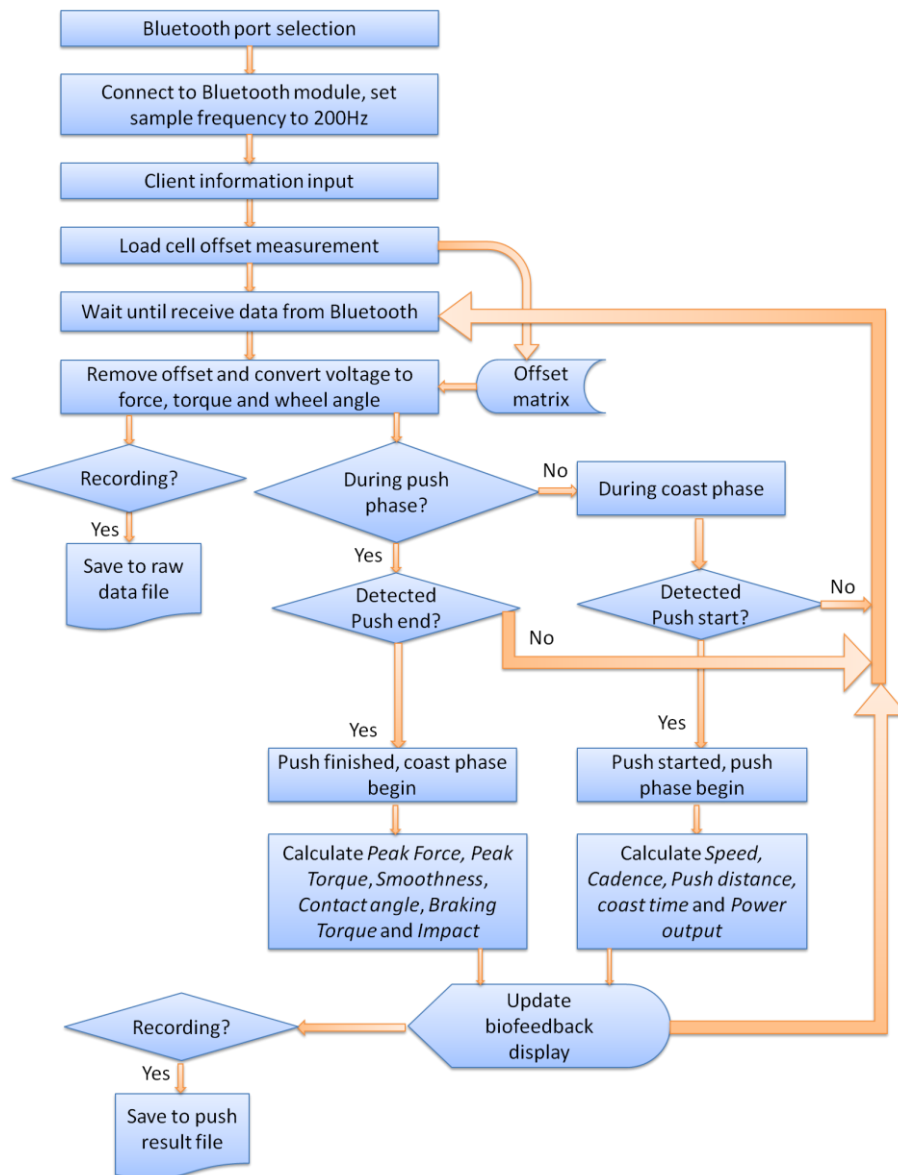


Figure 2.10 Flowchart of the OptiPush software

2.2.1 Bluetooth setting

A Bluetooth adapter is plugged into a computer to communicate with the Bluetooth module in the OptiPush Wheel. After connecting to the OptiPush module, the computer can control the wheel wirelessly. Once a “start” command is received from the computer, the module begins taking data at a sampling frequency of 200Hz and transferring them to the computer immediately. Raw data are recorded as 16-bit binary ranging from 0 to 65535 (representing 0-5V). Equation 2.10 is used to converter the raw data to voltage output.

$$Volt = \frac{raw\ data}{65535} \cdot 5V \quad (2.10)$$

2.2.2 Offset Removing

As the OptiPush Wheel rotates, the load cell coordinate system also rotates, resulting in a dynamic offset due to the weight of the handrim[23]. The load cell also has an offset due to the error of the electrical components and the weight of the beams to which the strain gauges are attached. To remove the offset, data recorded during a free rotation of the wheel are measured, averaged and subtracted from the propulsion data.

The OptiPush Software converts raw voltage measurements from the encoder to wheel angle using Equation 2.11.

$$Wheel\ angle = \frac{Volt}{5V} \cdot 360^\circ = \frac{raw\ data}{65535} \cdot 360^\circ \quad (2.11)$$

Wheel angle is rounded to the nearest integer angle from 0° to 359°. The software prompts the user to rotate the wheel without loading the handrim. A red circle is shown to represent the wheel and a needle indicates the current direction of the wheel (Figure 2.11). As the wheel is rotated, the red dots on the circle turn green as the system records three measurements of handrim loading at each wheel angle. After the entire circle is green, the loads at each wheel angle are averaged and a 7 x 360 matrix is saved to the offset file.

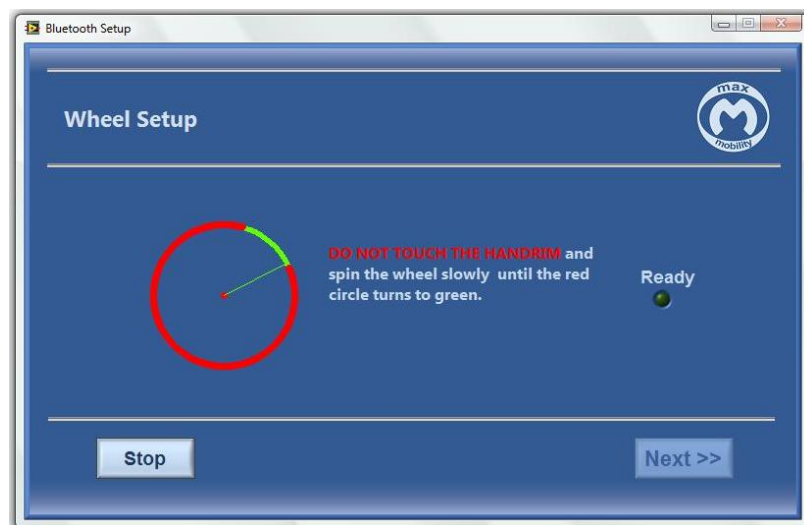


Figure 2.11 Offset data collection.

Data in the offset file is subtracted from all subsequent data before it is converted into handrim forces and torques. An example of offset data, from the in second column of the offset file, is shown in Figure 2.12.

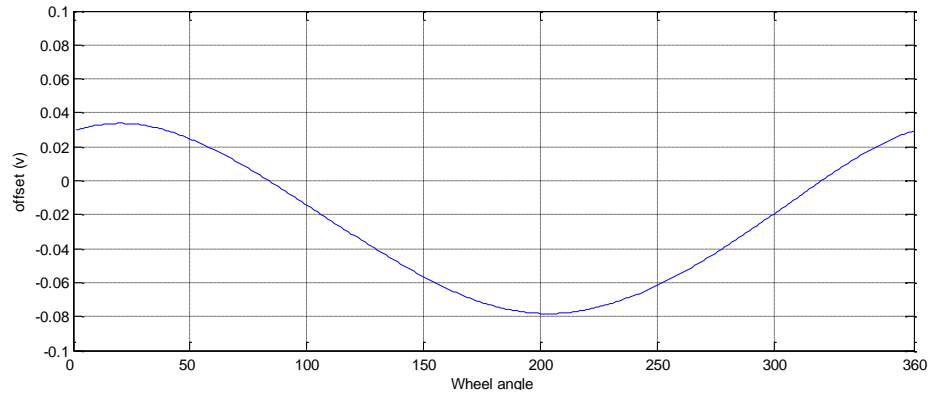


Figure 2.12 An example of offset data.

2.2.3 Variables

The OptiPush Software uses measurements of 3D forces and torques, and wheel angle, to calculate braking torque, cadence, contact angle, impact, peak force, peak torque, power output, push distance, coast time, smoothness and speed. All forces and moments are filtered by a 20-Hz, 4th order Butterworth low-pass filter and all variables are calculated on a stroke-by-stroke basis. Each stroke consists of a push phase followed by a coast phase. The push phase is defined as the period that absolute torque around the wheel axle is greater than 1Nm. The coast phase is defined as the period starting when the wheel torque was below 1 Nm and lasting until the start of next push phase (Figure 2.13).

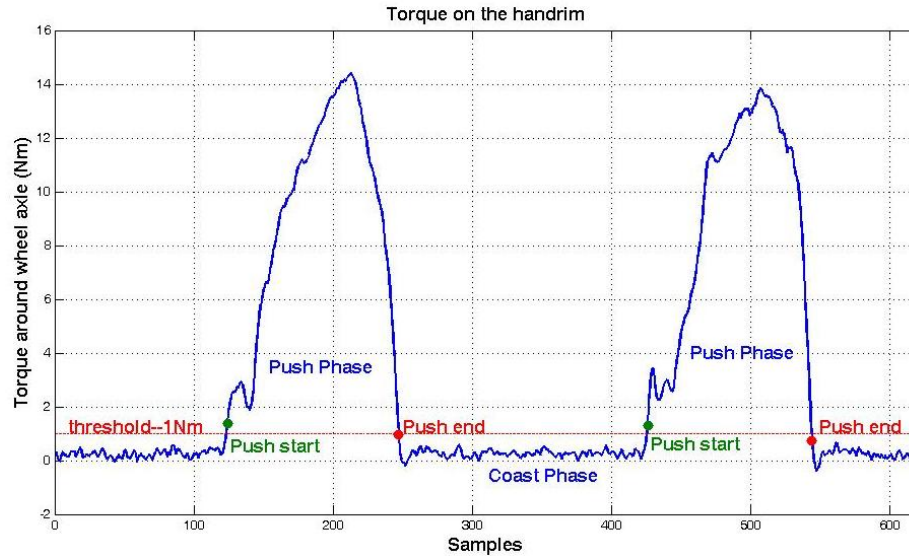


Figure 2.13 The push and coast phases of the stroke.

1) Braking Torque

Braking torque is defined as the maximum negative torque about the wheel axle for each push (Figure 2.14). When wheelchair users grasp the handrim, their hand speed is typically slower than the handrim rotating speed. This will slow down the wheelchair and cause a negative torque about the wheel axle. The greater the braking torque, the less efficient the grasp.

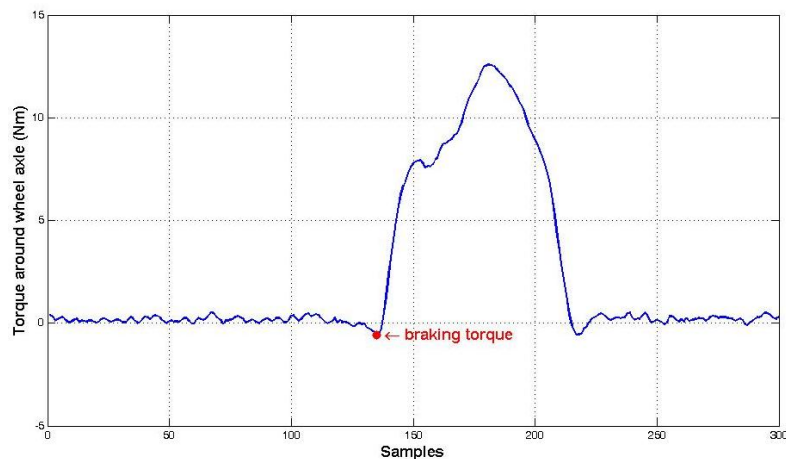


Figure 2.14 Braking torque.

2) Cadence

Cadence is defined as the push frequency in pushes per minute. A typical push frequency is around 1Hz, or 60 push per minute[24]. Some researchers have found that wheelchair users who push with a higher frequency are more likely to show symptoms of UE injury[24;25]. Cadence is calculated as:

$$Cadence_n = \frac{60}{t_{n+1} - t_n} \quad (2.12)$$

where t_n and t_{n+1} are the start times of the nth and (n+1)th push.

3) Contact Angle

Contact angle is defined as the change in wheel angle from the start of the push phase push to the end of the push phase. Users who push with higher cadence typically use a smaller contact angle. Since cadence has been associated with UE injuries, it is assumed that increasing contact angle will decrease cadence. Thus, contact angle has a potential role in improving propulsion technique. Contact is calculated as:

$$Contact\ angle_n = angle_{push\ end_n} - angle_{push\ start_n} \quad (2.13)$$

4) Impact

Impact is defined as the maximum rate of force loading. Impact is an important variable since it has also been associated with incidence of wrist injury[24]. Wheelchair users who exhibited greater impact were statistically more likely to develop wrist injuries[24]. Impact is calculated as:

$$Impact_n = Max\left(\frac{dF}{dt}\right) \quad (2.14)$$

where F is the resultant force applied to the handrim.

5) Peak Force

Peak force is defined as the maximum force magnitude applied to the handrim for each push during propulsion. As with impact, peak force has been found to be a predictor of wrist injury[26]. Peak force is calculated as:

$$Peak\ Force = Max\left(\sqrt{F_x^2 + F_y^2 + F_z^2}\right) \quad (2.15)$$

6) Peak Torque

Peak torque is defined as the maximum moment applied to the handrim for each push during propulsion. Peak torque is calculated as:

$$Peak\ Torque = Max\left(\sqrt{T_x^2 + T_y^2 + T_z^2}\right) \quad (2.16)$$

7) Power Output

Power output is defined as the average power generated during the push. Power output reflects the wheelchair user's pushing environment. Higher speed and rolling resistance require more power output. Power output is calculated as:

$$Power\ output = \frac{Energy}{Push\ Time} = \frac{\sum_{t_n}^{t_{n+1}}(T_z \cdot \Delta angle)}{t_{n+1} - t_n} \quad (2.17)$$

8) Push distance

Push distance is defined as distance travelled from the start of a push to the start of the next push. Usually, longer push distance comes with result of lower cadence which may reduce the change of UE injury. Push distance is calculated as:

$$Push\ distance = \frac{(angle_{push\ start_{n+1}} - angle_{push\ start_n}) \cdot D \cdot \pi}{360^\circ} \quad (2.18)$$

where D is the diameter of the wheel.

9) Coast Time

Coast time is defined as time from end of push to the start of next push and is also referred to as the recovery phase. It is the time when the hand is off the handrim and the UE is moving backwards in preparation for the next push. Coast time is calculated as:

$$Coast\ time = t_{push\ end_n} - t_{push\ start_{n+1}} \quad (2.19)$$

10) Smoothness

Smoothness is defined as ratio of the average force of a push to the peak force of a push. A higher ratio indicates the peak force is close to the average force, which translates to higher smoothness. Smoothness is calculated as:

$$Smoothness = \frac{\frac{\sum_{push\ start_n}^{push\ end_n} F}{t_{push\ end_n} - t_{push\ start_n}}}{peak\ force} \quad (2.20)$$

11) Speed

Speed is defined as the average speed of a push. Researchers often provide speed biofeedback to test subjects so that wheelchair users can maintain a certain speed[20;21]. Speed is calculated as:

$$Speed = \frac{push\ distance}{t_{push\ start_{n+1}} - t_{push\ start_n}} \quad (2.21)$$

2.2.4 Biofeedback

The OptiPush Software provides visual biofeedback for all variables (Figure 2.15). The variable pull-down menu on the top left can be used to select which variable is displayed on the upper plot, in which each bar represents the

value of the selected variable for a single push. The plot also includes a red line showing the average value of the variable over the 5 most recent pushes. The value of the most recent push is shown in the box labeled *Current Push*. A target value for the current variable can be set in the box labeled *Target* or by dragging the green line on the plot to the desired magnitude. For cadence, a metronome beep can also be used to help users reach a target push frequency.

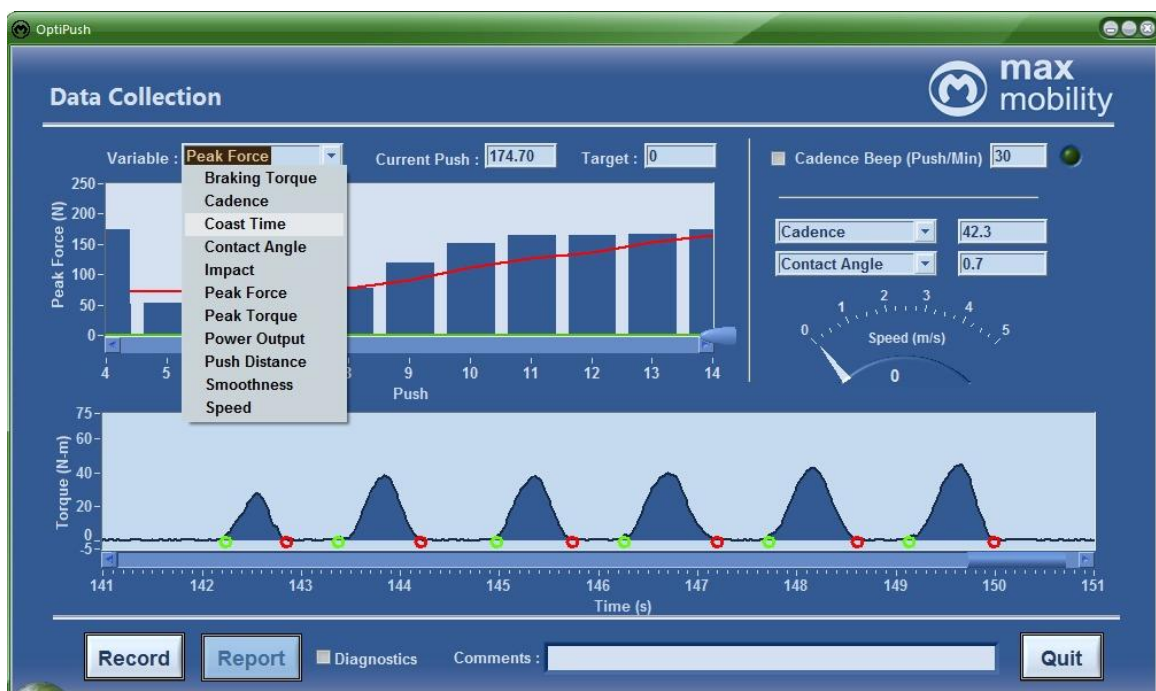


Figure 2.15 OptiPush Software interface.

2.3 System validation

The OptiPush Biofeedback System was validated for its force, torque, wheel angle and speed measurements using a multi-grade research treadmill (belt width: 1.06m; belt length: 5.69m). The treadmill level can be adjusted from -6° to $+6^\circ$ and includes safety straps to prevent wheelchair users from veering

off the belt and from tipping backwards during use. The straps run along linear bearings so as not limit movement or increase roiling resistance.

2.3.1 Wheel angle validation

A wheelchair with the OptiPushWheel attached to the right side was secured to the treadmill. The treadmill ran at a constant speed of about 0.7 m/s. The revolutions of the wheel were counted while the OptiPush Software recorded wheel angle. The treadmill was stopped after 100 revolutions were counted and wheel orientation at the stop position was measured. The resulting error in the wheel angle measurement was:

$$wheel\ angle = 360^\circ \times revolutions + angle_{stop} = 360^\circ \times 101 + 136.7^\circ = 36496.7^\circ$$

$$measured\ wheel\ angle = angle_{stop} - angle_{start} = 36675.5^\circ - 185.8^\circ = 36489.7^\circ$$

$$error = \left(\frac{measured\ wheel\ angle}{wheel\ angle} - 1 \right) \times 100\% = 0.02\%$$

2.3.2 Speed validation

Wheelchair speed is calculated using push distance (Equations 2.18 and 2.21), which is determined from wheel angle and wheel diameter. Given the previous validation of wheel angle, experimental calculations of wheel diameter were made to validate speed.

$$Push\ distance = \frac{(angle_{push\ start_{n+1}} - angle_{push\ start_n}) \cdot Dia \cdot \pi}{360^\circ} \quad (2.18)$$

$$speed = \frac{push\ distance}{Time_{push\ start_{n+1}} - Time_{push\ start_n}} \quad (2.21)$$

A wheelchair with an OptiPush Wheel attached was secured to the treadmill. To simulate typical wheelchair loading, an 85-kg adult male sat in the wheelchair. The treadmill was set to run at about 1m/s. The revolutions of treadmill belt and wheel were counted for each of the 5 different OptiPush Wheel diameters (20 in, 22 in, 24 in, 25 in, and 26 in). All tires were inflated to the manufacturer's recommended pressure of 110 pounds per square inch (psi). Wheel diameter (D) was calculated as:

$$D = \frac{\text{Revolutions of belt} \times \text{belt length}}{\text{Revolutions of wheel}} \quad (2.22)$$

Each size of wheel was tested twice. Error was calculated as the difference between the two measurements of diameter divided by average of two measurements, multiplied by 100. Results are shown in Table 2.1.

Table 2.1 Results of wheel diameter testing at a tire pressure of 110 psi

Wheel Size (inch)	Rev. of treadmill belt	Rev. of wheel	Dia (m)	Error (%)
20	9-3.5/224.1	33+20/360	1.5468	-0.04
	8+14.0/224.1	29+235/360	1.5474	
22	9+5.6/224.1	30+85/360	1.6987	0.02
	9-1.3/224.1	30+50/360	1.6984	
24	10+5.3/224.1	31+90/360	1.8254	0.04
	10+5.5/224.1	31+95/360	1.8248	
25	10+1.2/224.1	30	1.8980	0.00
	10+9.5/224.1	30+40/360	1.8980	
26	10+21.5/224.1	29+5/360	1.9803	-0.04
	10-9.0/224.1	28+220/360	1.9811	

Wheel diameter of the smallest (20 in) and largest wheel (26 in) were retested at tire pressure of 90 psi. Error was calculated as the difference between

the two measurements of wheel diameter (110 psi and 90 psi) divided by the initial measurement of wheel diameter (110 psi), multiplied by 100. The results are shown in Table 2.2.

Table 2.1 and Table 2.2 show that the maximum error in wheel diameter for the 110 psi and 90 psi conditions is about 0.04% and -0.77%, respectively. Therefore, tire pressure has little effect on wheel diameter a little. By combining the results from the tests of wheel angle and wheel diameter, the maximum error in wheel speed was found to be 0.08% for a tire pressure of 110 psi and 0.81% for a tire pressure of 90 psi.

Table 2.2 Results of wheel diameter testing at a tire pressure 90 psi

Wheel size (inch)	Rev. of treadmill belt	Rev. of wheel	Dia (m)	Error (%)
20	8+7/224.1	29+220/360	1.5435	-0.21
	8-1/224.1	29+200/360	1.5396	-0.50
26	10+7.3/224.1	28+325/360	1.9754	-0.25
	10-9/224.1	28+300/360	1.9658	-0.77

2.3.3 Force and Torque validation

Static and dynamic tests were performed to validate the 3D force and torque measurements from the load cell. For static testing, forces along the fore-aft (F_x) and superior-inferior (F_y) axes and torque about the medial-lateral (T_z) axis were tested by mounting the OptiPush wheel vertically. Three reference loads (23.28 N, 68.04 N and 109.99 N) were suspended from the handrim at eight different wheel angles (45° apart) such that the resultant force of F_x and F_y

will be the weight of load (Figure 2.16a). The two smaller loads (23.28 N and 68.04 N) were suspended on the handrim such that the suspending point of the load was at the center of the wheel, creating a T_z equal to the weight of load multiplied by radius of handrim (Figure 2.16b).

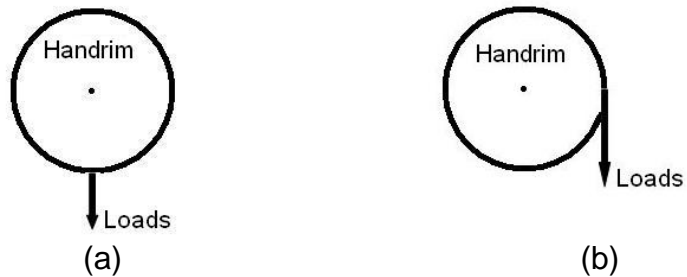


Figure 2.16 Load applied to the handrim for testing (a) F_x , F_y and (b) T_z .

Force along the medial-lateral (F_z) axis and the torques about the fore-aft (T_x) and superior-inferior (T_y) axes were tested by mounting the OptiPush wheel horizontally. Three reference loads (23.28 N, 68.04 N and 109.99 N) were suspended from the beams to test F_z . The smaller two loads (23.28 N and 68.04 N) were then suspended from the handrim such that the resultant torque of T_x and T_y equaled the weight of load multiplied by radius of handrim.

More than 10 seconds of data was collected for the different loads and positions. The error in each force and torque measurement was calculated by:

$$Error = \frac{\text{average of measured result} - \text{reference result}}{\text{reference result}} \times 100\% \quad (2.23)$$

The resulting averages and standard deviations of the errors are shown in Tables 2.3 through 2.7. Overall, the maximum absolute error in force was 3.8%, and the maximum absolute error in torque was 2.04%.

Table 2.3 Results for testing F_x and F_y with a reference load of 23.28N

Position (°)	Average (N)	Standard deviation(N)	Error (%)
0	23.11	1.59	-0.74
45	23.75	1.66	2.02
90	22.94	1.21	-1.48
135	24.04	1.63	3.24
180	23.85	1.47	2.43
225	23.38	1.68	0.41
270	22.75	1.34	-2.28
315	22.40	1.89	-3.8

Table 2.4 Results for testing F_x and F_y with a reference load of 68.04N

Position (°)	Average (N)	Standard deviation(N)	Error (%)
0	66.55	1.65	-2.19
45	67.05	1.74	-1.45
90	66.26	1.53	-2.62
135	67.39	1.35	-0.96
180	67.08	1.50	-1.42
225	66.65	1.75	-2.05
270	65.84	1.42	-3.23
315	65.51	1.64	-3.72

Table 2.5 Results for testing F_x and F_y with a reference load of 109.99N

Position (°)	Average (N)	Standard deviation(N)	Error (%)
0	108.68	1.47	-1.19
45	109.17	1.47	-0.75
90	108.25	1.35	-1.59
135	109.45	1.44	-0.49
180	109.23	1.70	-0.69
225	108.92	1.59	-0.97
270	107.78	1.41	-2.01
315	107.43	1.57	-2.33

Table 2.6 Results for testing F_z

Reference Loads (N)	Average (N)	Standard deviation(N)	Error (%)
23.28	23.31	3.20	0.10
68.04	66.49	3.74	-2.28
109.99	112.66	3.16	2.42

Table 2.7 Results for testing torque

Variable	Ref. Loads (Nm)	Average (Nm)	Standard deviation (Nm)	Error (%)
$T_x + T_y$	6.03	5.99	0.09	-0.56
	17.61	17.45	0.10	-0.89
T_z	6.03	6.08	0.07	0.87
	17.61	17.97	0.07	2.04

Dynamic testing was done to further validate F_x , F_y , and T_z under more realistic conditions. The OptiPush Wheel was attached to the right side of a wheelchair that was secured to the treadmill. One at a time, two reference loads (1.174 kg and 2.296 kg) were attached to the handrim (Figure 2.17). Each load condition was tested at three different treadmill speeds (0.5 m/s, 1.0 m/s and 1.5m/s).

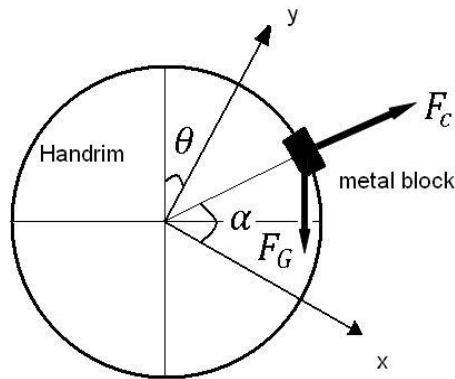


Figure 2.17 Centrifugal force (F_C) and gravity (F_G) of the metal block applied to the handrim for dynamic testing; where θ is wheel angle and α is the angle of metal block.

Because the wheel was mounted vertically, the load did not generate force or torques perpendicular to the wheel (F_z , T_x , T_y). The planar forces (F_x and F_y) and torque (T_z) were calculated by the following equations:

$$\begin{cases} F_x = F_G \cdot \sin(\theta) + m \cdot \omega^2 \cdot r \cdot \cos(\alpha) \\ F_y = -F_G \cdot \cos(\theta) + m \cdot \omega^2 \cdot r \cdot \sin(\alpha) \\ T_z = F_G \cdot \cos(\theta - \alpha) \cdot r \end{cases} \quad (2.24)$$

where ω is the angular velocity of wheel; r is the radius of handrim and m is the mass of the metal block.

Force, torque and wheel angle data were collected for more than 10 wheel revolutions, for each load, at 3 different treadmill speeds. These values were compared to the reference forces and torques calculated from Equation 2.24. Figure 2.18 shows the measured F_x compared with reference F_x and Figure 2.19 shows the measured T_z compared with reference T_z .

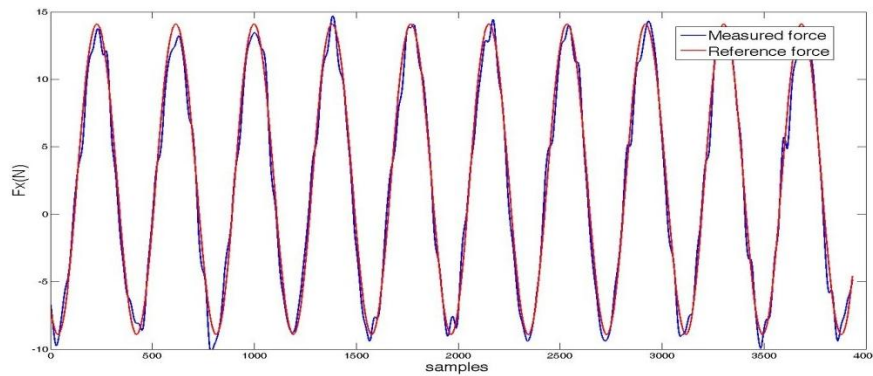


Figure 2.18 Measured F_x and reference F_x at a treadmill speed 1.0m/s with 1.174 kg metal block attached to the handrim.

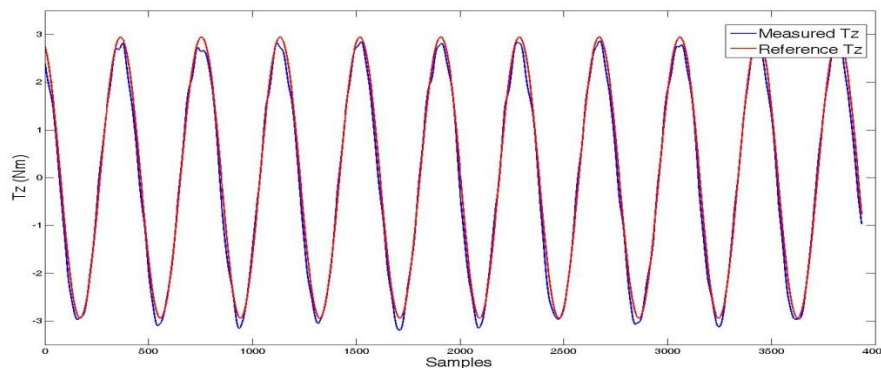


Figure 2.19 Measured T_z and reference T_z at a treadmill speed of 1.0m/s with a 1.174 kg metal block attached to the handrim.

Correlations between the reference and measured results were also calculated along with the average and standard deviation (STD) of the errors

between the two sets of values. Table 2.8 lists the differences between the measured and calculated values of F_x , F_y , and T_z for each load and speed condition. The measured results were found to be highly correlated ($r > .985$) with the reference results. The average error in force ranged from -0.96 N to 0.83 N and the average error in torque ranged from 0.10 Nm to 0.14 Nm.

Table 2.8 Results of dynamic testing

Loads (kg)	Speed (m/s)	Measure	Correlation Coefficient	Avg Error (N)	STD Error (N)
1.1737	0.5	F_x	0.989	-0.04	1.20
		F_y	0.988	-0.20	1.32
		T_z	0.999	0.13	0.08
	1.0	F_x	0.994	0.31	0.93
		F_y	0.993	-0.60	1.03
		T_z	0.997	0.13	0.17
	1.5	F_x	0.994	0.42	0.92
		F_y	0.993	-0.81	1.16
		T_z	0.986	0.11	0.35
2.2963	0.5	F_x	0.998	0.11	1.31
		F_y	0.997	-0.28	1.25
		T_z	0.999	0.14	0.11
	1.0	F_x	0.998	0.83	1.22
		F_y	0.998	-0.96	1.03
		T_z	0.998	0.14	0.26
	1.5	F_x	0.997	0.69	1.36
		F_y	0.995	-0.60	1.55
		T_z	0.998	0.10	0.25

2.4 Conclusion

The OptiPush Biofeedback System is a powerful research tool for studying wheelchair propulsion technique. It wirelessly measures 3D forces and torques applied to the handrim, along with the wheel angle during push. The modular design of the instrumentation allows the device to incorporate 5 different wheel

sizes. The accompanying software calculates handrim loading and provides biofeedback variables to wheelchair users. In validation tests, the system demonstrated low measurement error in all forces and torques. Overall, the functionality and accuracy of the system make it valid and useful in studies of wheelchair propulsion.

CHAPTER III

TESTING THE OPTIPUSH BIOFEEDBACK SYSTEM

The OptiPush Biofeedback system is designed for studying manual wheelchair propulsion technique and training wheelchair users. However, before developing a training protocol or testing the effects of the biofeedback, we tested the viability of OptiPush biofeedback system. We hypothesized that wheelchair users would be able to: 1) interpret the biofeedback and make significant and targeted changes to the variables, and 2) hit specific, $\pm 10\%$ change of the nominal value as targets for select variables.

3.1 Methods

3.1.1 Participants

Thirty-one individuals were enrolled in this study. To be enrolled, individuals had to use a manual wheelchair as their primary mode of transportation, have complete function and sensation in the upper limbs, have no upper limb pain that would impair propulsion, be able to propel for periods of up to 5 minutes at a time, and use a manual wheelchair equipped with quick-release rear wheels. Prior to enrollment, all participants were required to provide

informed consent. All study documents and test procedures were approved by the Western Institutional Review Board (Olympia, WA).

3.1.2 Data Collection

The rear wheels of each participant's wheelchair were removed and replaced with an OptiPush wheel on the right side and an inertia-matched dummy wheel on the left. Both wheels were the same diameter as the participant's normal rear wheels. With the testing wheels attached, participants were asked to propel their wheelchair across a low-pile carpet to obtain nominal propulsion data. Data from two trials, run in opposite directions across the floor, were processed by the OptiPush software to determine speed, cadence, and power output on a stroke-by-stroke basis. Participants were then loaded onto the research treadmill and secured to the frame by attaching the two safety straps to the front of the wheelchair. The speed of the treadmill was set to match each participant's mean overground speed and the grade was set to elicit the same power output as overground propulsion. Participants were given several minutes to get acclimated to pushing on the treadmill. During this time, participants were also told to try to match their cadence to a metronome set to beep at their average overground cadence. Once participants were comfortable, a control (normal propulsion) trial was captured. The trial lasted approximately 1 minute. Wheel angle and the 3D forces and torques applied to the handrim were recorded by the OptiPush Software. The mean speed, cadence, and power output of the trial were checked against the overground means to ensure

similarities. If necessary, adjustments were made to the treadmill and the trial was redone. The control trial served as the reference against which all biofeedback trial results were compared.

3.1.3 Single-Variable Biofeedback

The OptiPush Software was set to display six biofeedback variables: two primary variables (cadence and peak force) and four secondary variables (braking torque, contact angle, push distance, and smoothness). Each of the primary variables have been linked to upper limb pain and injury[35], while the secondary variables may provide users with an alternate means of preserving upper limb health. Targets were created for each biofeedback variable based on the clinical practice guideline(CPG) recommendations[35]: Use long, smooth strokes that limit high impacts on the pushrim. The goal of each target was to reduce strain on the upper limb by reducing cadence and force. Depending on the variable, this was targeted directly (primary variables) or indirectly (secondary variables). Participants were asked to decrease cadence, peak force, and braking torque, and to increase contact angle, push distance, and smoothness. For most variables, two targets were set: an extreme change (minimize or maximize the variable) and a subtle change ($\pm 10\%$ of the nominal value). A 10% change seemed like a reasonable target for a future propulsion training program. Braking torque and smoothness do not typically have large margins for change; therefore, participants were asked only to improve each variable as much as possible. Table 3.1 provides the testing target for each variable.

Table 3.1 Targets for biofeedback variables

Variable	Target(s)	
Cadence	Minimize cadence	reduce by 10%
Peak Force	Minimize peak force	reduce by 10%
Braking Torque	Minimize braking torque	N/A
Contact Angle	Maximize angle	increase by 10%
Push Distance	Maximize distance	increase by 10%
Smoothness	Maximize smoothness	N/A

For each biofeedback condition, participants were shown a bar graph displaying the stroke-by-stroke magnitude of a single variable on a monitor in front of the treadmill (Figure 3.1a). The display also included a red 5-stroke average line to help with targeting. Participants were asked to alter their propulsion technique in order to change the height of the bars to reach each target. For the minimize/maximize conditions, participants were asked to make as great a change as possible, while keeping the height of each bar about the same as the previous bars. For the 10% target conditions, a green target line was displayed over the bar graph. Participants were asked to match the height of each bar to the height of the target line, or in other words, to match the red 5-stroke average line to the green target line (Figure 3.1b). To help the participants understand what they needed to do to change each variable, we described the possible changes in propulsion technique. For example, we explained that to reduce peak force, users could increase contact angle, increase cadence, or possibly increase fraction of effective force[19].

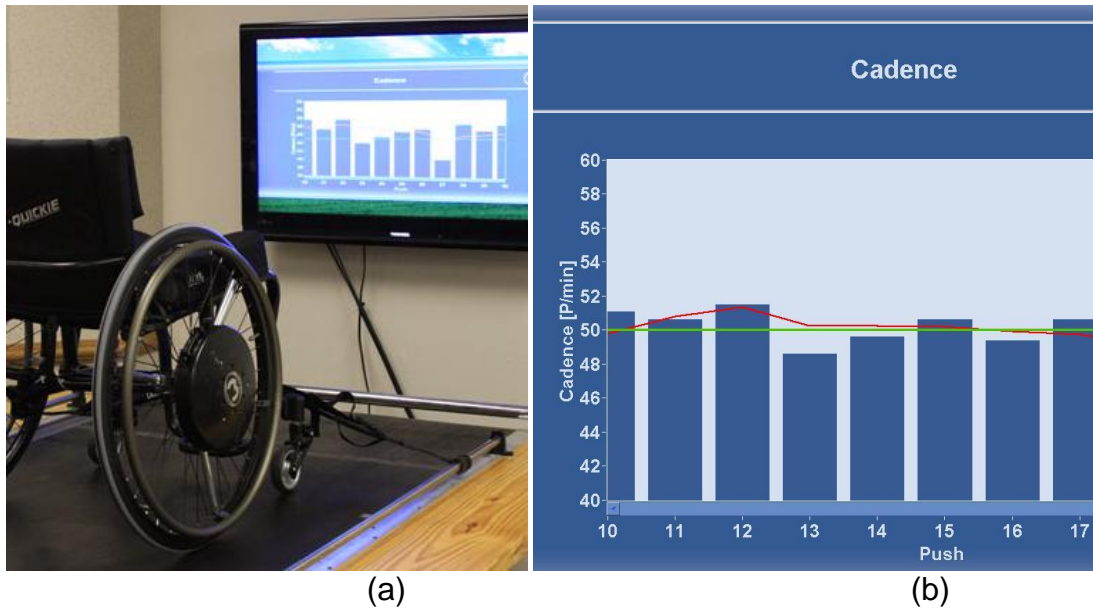


Figure 3.1 The testing setup (a) and biofeedback display (b) used in this study.

Variables were selected and presented in a randomized order. Within each variable, the minimize/maximize condition was run first and the 10% change condition second. This was done to help participants get more comfortable responding to the variable before attempting the more controlled 10% change condition. Participants were given 30-90 seconds to adapt their technique enough to reach each target. Once they had approximately reached the target, data collection was started. OptiPush data were recorded for 1 minute. In the event that the participant could not understand the variable or how to adjust its value, further explanation was provided and the trial was repeated. Participants were given several minutes to rest in between each trial to avoid fatigue.

3.1.4 Data Analysis

For each condition and each participant, the value of the biofeedback variable was averaged across all strokes and compared to the mean control variable. This yielded the mean relative change (%) of each variable. The relative changes were analyzed with a series of independent samples t-tests. To account for the 10 individual comparisons, alpha was adjusted to .005.

3.2 Results

3.2.1 Participants

Thirty-one manual wheelchair users (27 males, 4 females) participated in the study. Twenty-three participants had paraplegia (T3-L1), 1 had tetraplegia (C6-7 incomplete), 6 had spina bifida (T10-L5), and 1 had cerebral palsy. On average, the participants were 34.1 ± 9.5 years old and had 15.0 ± 10.2 years of manual wheelchair experience. Table 3.2 shows the mean variables for normal wheelchair propulsion (control trial) on the treadmill.

3.2.2 Viability of Biofeedback

For each feedback condition, mean speed decreased, but remained within 0.5% of normal propulsion speed. Changes in power output were less than 5% (0.45% - 4.93%), except for the 'Maximize Contact Angle' condition, in which the power output increased 7.82%. Table 3.3 shows the percent change in each variable between the biofeedback condition and the control trial. For nine of the

eleven conditions, participants were able to significantly ($p < .005$) improve the value of the biofeedback variable. Participants exhibited good control over cadence, push distance, and especially, contact angle. For the 10% target condition, the mean contact angle error was 0.07% and the standard deviation was the smallest (4.4%) of any condition. On the other hand, participants had difficulty making significant changes to peak force and smoothness. At most, they were able to decrease peak force an average of 11.37%. Although this was greater than the -10% target set for the following trial, they were unable to reach the target, reducing peak force by only 3.9%. A similarly small increase and high variability were seen in smoothness for the 'Maximize Smoothness' condition.

Table 3.2 Normal propulsion variables

Variable	Value
Speed	1.10 (0.23) m/s
Power Output	8.52 (2.50) W
Treadmill Angle	0.82 (0.27) degrees
Braking Torque	0.80 (0.37) Nm
Contact Angle	87.03 (17.79) degrees
Cadence	52.41 (10.88) strokes/min
Push Distance	1.33 (0.41) m
Peak Force	57.38 (12.93) N
Smoothness	0.67 (0.05)

Values are mean (standard deviation [SD])

Table 3.3 Changes to the target variable during each biofeedback condition

Variable	Condition	Actual change (%)
Braking Torque	Minimize	-43.50 (28.10)*
Contact Angle	Increase by 10%	10.07 (4.40)*
	Maximize	31.43 (21.51)*
Cadence	Decrease by 10%	-9.48 (5.17)*
	Minimize	-63.59 (13.73)*
Push Distance	Increase by 10%	10.52 (6.83)*
	Maximize	254.5 (135.9)*
Peak Force	Decrease by 10%	-3.91 (8.79)
	Minimize	-11.37 (16.87)*
Smoothness	Maximize	2.10 (7.70)

Values are mean (SD); *p < .005

3.3 Discussion

In general, participants were able to interpret the biofeedback and make significant and targeted changes to the variables by using OptiPush Biofeedback System. The results showed that participants had the potential to make significantly large changes to their braking torque, cadence, and push distance. The magnitude of these changes (43-250%) suggest that users might be able to make smaller, though still significant, changes in these variables with less effort or attention. This is particularly relevant to cadence, which has been linked to UE injury. Perhaps subtle changes in propulsion technique can reduce cadence and the risk of injury. For the 10% target conditions, participants demonstrated good control over cadence, contact angle, and push distance. The actual change

made to each variable was within 0.52% of the target. In particular, the accuracy and precision with which changes were made to contact angle were impressive.

Peak force and smoothness were the two variables that proved difficult to change. Both variables describe the peak force on the handrim, either directly or as a ratio of average force to peak force (smoothness), and thus, both are susceptible to the high variability of force across strokes. A calculation of the coefficient of variation (standard deviation divided by the mean) showed the changes in peak force and smoothness to be the most variant of all the biofeedback variables (Table 3.4). Participants were able to significantly ($p < 0.005$) decrease peak force during the 'Minimize Peak Force' condition; however, the 11.37% change was small compared to those made to the other biofeedback variables, and a similar decrease could not be replicated in the following 'Decrease Peak Force by 10%' condition. A breakdown of the data from the latter condition (Table 3.5) revealed three distinct performance groups: decreased peak force by more than 9% ($n = 10$), decreased peak force by less than 9% ($n = 10$), and increased peak force ($n = 10$). Data collected from one participant was unusable. Participants in the third group actually increased peak force (1.29-20.97%). Three groups were also defined for the 'Minimize Smoothness' condition: increased smoothness by at least 2% ($n = 13$), no change (-2% to +2%) in smoothness ($n = 10$), decreased smoothness at least 2% ($n = 8$). Five of the eight participants who decreased smoothness also increased peak force for the peak force target condition. These findings demonstrate the difficulty in reducing peak force as well as the difficulty in hitting a specific peak force-based targets.

Table 3.4 Coefficient of variation (CV) for each biofeedback variable

Variable	Condition	CV
Braking Torque	Minimize	0.646
Contact Angle	Increase by 10%	0.437
	Maximize	0.684
Cadence	Decrease by 10%	0.545
	Minimize	0.216
Push Distance	Increase by 10%	0.649
	Maximize	0.534
Peak Force	Decrease by 10%	2.248
	Minimize	1.484
Smoothness	Maximize	3.667

Table 3.5 Breakdown of force data from the ‘Decrease Peak Force by 10%’ and ‘Maximize Smoothness’ conditions

Group	Decrease Peak Force by 10%		Maximize Smoothness	
	Number of participants	Mean change in Peak Force (%)	Number of participants	Mean change in Smoothness (%)
1	10	-12.19 (1.96)	13	9.23 (5.27)
2	10	-6.12 (1.90)	10	-0.53 (1.02)
3	10	6.57 (6.17)	8	-6.42 (4.35)

Values are mean (SD).

Unlike other propulsion variables, peak force represents a single, unconstrained point in the stroke. Therefore, peak force can occur at any part of the stroke and can change location as the user makes adjustments to propulsion

technique. This likely increases the difficulty for manual wheelchair users to control its value. To help manual wheelchair users make more significant reductions in peak force, additional feedback may be necessary.

3.4 Conclusions

Biofeedback is an effective method of generating improvements in manual wheelchair handrim biomechanics. Participants were able to use the biofeedback provided by OptiPush to make significant and controlled changes to cadence, push distance, and contact angle. Significant changes were also made to braking torque and peak force; however, the improvements in peak force were limited and variable. Additional or altered biofeedback is needed to help users increase smoothness and decrease peak force.

CHAPTER IV

MULTIVARIABLE BIOFEEDBACK DESIGN & TESTING

By studying on the effects of single-variable biofeedback, we observed the ability of subjects to make both large and targeted changes in a number of propulsion variables, including braking moment, cadence, contact angle, peak force and push distance and smoothness. Using a real-time, stroke-by-stroke bar graph, subjects were able to make significant changes to each biofeedback variable, except for smoothness. Subjects could only increase smoothness by 2%, but in attempting to maximize smoothness, they decreased braking moment (-20%), cadence (-9%) and impact (-7%), while increasing contact angle (6%) and push distance (15%). These types of cross-variable interactions allowed users to make improvements across multiple variables without having to actively monitor each variable. Unfortunately, no test condition resulted in indirect improvements to peak force. Peak force could only be reduced when it was the biofeedback variable, and even then, the improvement was relatively small (11% decrease). The modest decrease in peak force (-11.3%) also came at the cost of cadence, which increased by 20%. While single-variable biofeedback can be beneficial for teaching some aspects of wheelchair use, like maintaining a safe speed, a multivariable approach is needed to address the negative tradeoffs and the difficulties in lowering peak force.

4.1 Multivariable biofeedback design

Biofeedback is a learning strategy deriving from psychological learning theory. Its theoretical basis is "operant conditioning" or "learning through reinforcement" in the tradition of B.F. Skinner [27]. In order to maximize the effectiveness of biofeedback, Mark Stephen Schwartz, et al. suggests minimizing the effort required from users [28].

The OptiPush single variable biofeedback interface provides push-to-push results as a bar chart to users. Some of the variables like speed and cadence were calculated from over the entire push-recovery cycle. Peak force and contact angle, however were calculated over the push phase only, allowing for a more immediate feedback of that information. While providing this information prior to the next push likely helped improve the user's ability to respond to it before engaging in the next push, peak force was still found to be difficult if not impossible for the majority of the users.

It was hypothesized that providing handrim force continuously over the push would allow the user to better identify with it and control it. There are many instances in the literature where continuous or moment-to-moment feedback was found to be an effective approach to either increase or decrease an individual's force production or muscle activity [29-33]. In particular, Steven Cohen, et al. compared the effect between continuous reinforcement (feedback) and

intermittent reinforcement for muscle activity training [34]. Their results showed that continuous feedback led to the best performance.

Based on these results, a time-based handrim force profile plot was developed that refreshed with each push. The approach to focus on one individual push at a time was chosen to maximize the visual scale of each push and to emphasize the current push. Internal testing among lab staff and select pilot users showed considerable promise in improving control of peak force. However, as was found in the single variable biofeedback results, efforts to decrease handrim force resulted in increases in cadence.

In an attempt to control both peak handrim force and cadence, the time-based force graph was positioned next to the bar chart biofeedback display used in the single variable study. The bar chart was set to cadence and the system was tested internally. The dual display of force and cadence was too complex to interpret. With the two independent displays of information, the tendency was to focus on one display or the other, but watching both was not possible for any of the internal testers. The results of this round of testing reinforced the need for biofeedback to minimize the effort required by the individual to interpret it [2].

It was further hypothesized that a biofeedback display that incorporated both handrim force and cadence information simultaneously would enable users to achieve the desired performance goals. To achieve this, a metronome beep was introduced to provide a cadence goal, while visually focusing on the time-based force graph. Our internal test group evaluated the new audio-visual biofeedback and found it to be much easier to follow than the dual-display

approach. However, it was easy to fall behind and lose timing with the prescribed frequency.

While the use of audio enabled both force and cadence to be conveyed simultaneously, the cadence was not actually biofeedback of the user's performance. It was simply a desired goal. As the user varied cadence, the metronome beep did not change in response. It was hypothesized that contact angle might be an effective surrogate to induce changes in cadence. Contact angle was found to be negatively correlated with cadence in the single variable study, so increases in contact angle resulted in decreases in cadence. Based on these results, a new approach was envisioned, where handrim force is plotted as a function of contact angle, rather than time. With this approach, the user would be presented with a force-spatial relationship, allowing the two biofeedback variables to coexist on the same graph.

Based on this idea, a new multi-variable biofeedback design was developed that combined force and contact angle (Figure 4.1). Each vertical bar represents the average force over each 3 degrees of contact angle. The bar graph calculates from push start to push end and refreshes at push start. The highest bar represents peak force. The number of bars indicates the contact angle of current push. From this interface, users can interpret at what wheel angle or at which position on the handrim the peak push force is reached. A horizontal target line was used to define the maximum acceptable peak force and a vertical target line was used to determine the smallest acceptable contact angle

for each push. Internal testing showed considerable promise and it was decided that this new biofeedback format should be formally tested to assess its efficacy.

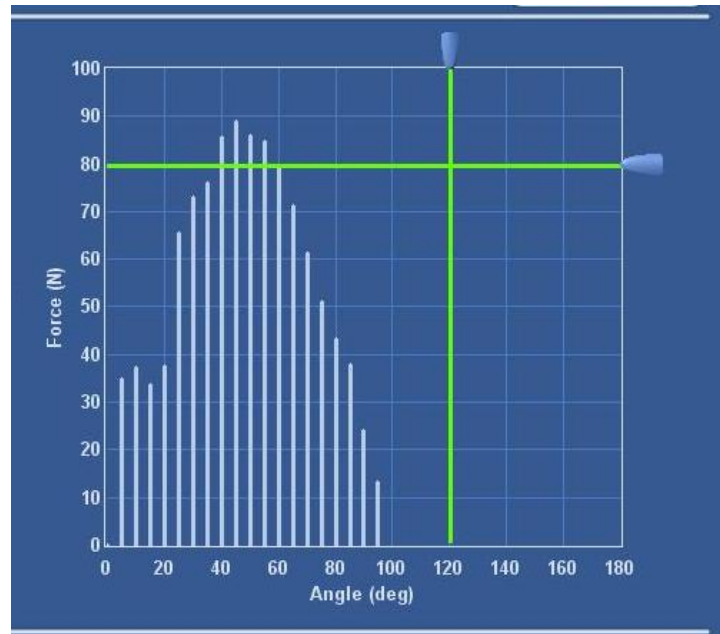


Figure 4.1 Multivariable biofeedback interface

4.2 Multivariable biofeedback testing

4.2.1 Subjects

Thirty-two full-time manual wheelchair users participated in this study. Subjects were recruited from an internal database and through local rehabilitation facilities. To qualify for participation, individuals were required to: use a manual wheelchair as their primary means of mobility; have no impairment, injury or lack of feeling in their upper limbs; be able to push for up to five minutes at a time; use a wheelchair with quick-release axles; and have no medical condition that

could be aggravated by propulsion or moderate exercise. All subjects provided written informed consent prior to enrollment; and all forms and testing procedures were approved by the Western Institutional Review Board (Olympia, WA).

4.2.2 Data Collection

Each subject completed several forms that addressed personal and injury information, including date of birth, date of injury, and level of injury. The weight of the subject and wheelchair were obtained with a wheelchair scale. The rear wheels were then replaced with a pair of OptiPush wheels, which can record wheel angle, wheel speed and the tri-axial forces and moments applied to the handrim at 200 Hz. Left and right side wheel data were recorded by two individual computers and they started recording data at same time by using an external trigger. Both wheels were the same diameter as the subject's own wheels (501mm - 590mm) and were fitted with low-profile tires inflated to 689 kPa (100 psi). Once the wheels were replaced, subjects were secured to a motor-driven treadmill with a pair of straps attached to the front of the wheelchair. The straps glide along rails on the side of the treadmill and keep the wheelchair from rolling off the belt while adding minimal rolling resistance. For all trials, the treadmill was set to a speed of 1.34 m/s and a grade of 0.5 degrees.

Testing began with a five minute warm-up period to allow subjects to get comfortable pushing on the treadmill. After a rest period of at least five minutes, a 1-minute normal propulsion trial was completed. During the trial, bilateral handrim biomechanics were recorded by the two OptiPush wheels. Data were filtered with

a 4th order Butterworth digital filter (20 Hz cutoff frequency) and segmented in push strokes based on moment about the axle. Conditioned force, moment and wheel angle measurements were used to compute 11 stroke-by-stroke variables. This investigation focused on 4 outcome variables: contact angle, cadence, peak force, impact; the latter three of which have been linked to signs of upper limbs injury[10;10-12]. The normal trial served as the baseline for all subsequent changes in handrim biomechanics.

Next, subjects watched an education video (Figure 4.2) that demonstrated the recommendations of the Clinical Practice Guideline (CPG) [35]. The video encouraged subjects to spread their push force over a large contact angle - a technique that can be used to reduce peak force and cadence while holding speed constant. The video also explained how approaching the handrim from below can help match the movement of the hand to the arc and rotation of the handrim. This enables users to reduce impact during initial contact and improve early push phase efficiency[36]. After watching the video, subjects attempted to push with longer, smoother, under-rim strokes[36]. Subjects were free to use either the semicircular or double loop stroke pattern. This education trial lasted up to 2 minutes. Subjects were given 1 minute to settle into their new push technique before bilateral handrim biomechanics were recorded for 1 minute.

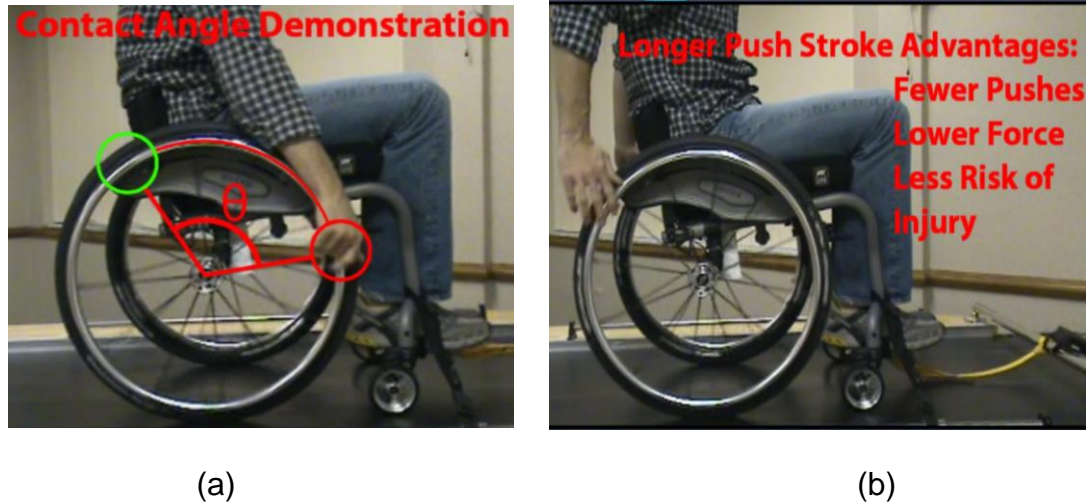


Figure 4.2 Education video that demonstrated (a) contact angle; (b) longer push stroke advantages.

Subjects then watched a second video describing the multivariable biofeedback display (Figure 4.3). The values of the target lines for the 2-D biofeedback were initially set to the average peak force and contact angle from each subject's normal propulsion trial. As testing progressed, the target lines were adjusted to promote further improvements after the subject had surpassed the former goals. Throughout the biofeedback trials, subjects were encouraged to achieve lower forces by spreading their pushes over a larger contact angle. This was an individualized process that included specific recommendations based on trial by trial observations and measurements. Table 4.1 lists the primary recommendations given to each subject. Beyond stressing the recommendations of the CPG (Table 4.1, points 1-3), subjects were advised to start the push stroke by pulling upward on the handrim before pushing forward. This can expedite the generation of a propulsive moment and help users get more out of the beginning of the push stroke. It can also eliminate the need for strong triceps contraction, or

“snapping” that some users tend to do near the end of handrim release. Subjects were also encouraged to sit upright and to avoid leaning forward throughout the trial. Based on pre-test results, we found that leaning forward tends to decrease contact angle and can lead to higher forces due to a greater percentage of weight on the casters.

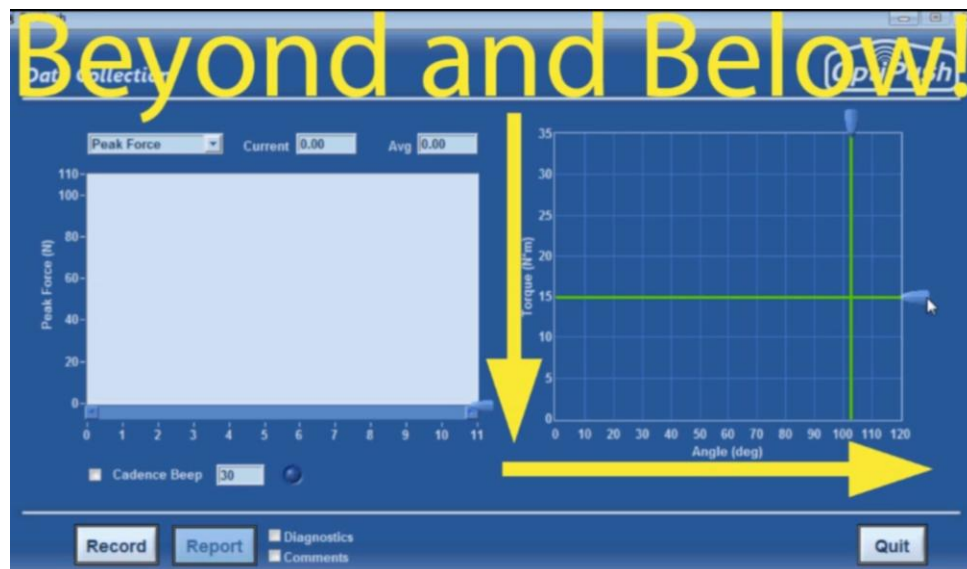


Figure 4.3 Optipush biofeedback video that shows the target of multivariable biofeedback

Table 4.1 Primary instructions/recommendations on how to improve handrim biomechanics

-
1. Use a long, smooth push stroke
 2. Spread push force over a large contact angle
 3. Approach the handrim from below
 4. Begin the push stroke by pulling up on the handrim
 5. Sit upright and avoid a forward leaning posture
-

When necessary, additional techniques were implemented to promote improvements. An auditory beep was used to help some subjects maintain improvements in cadence. For those who had difficulty reducing peak force, efforts were first focused on minimizing cadence without increasing peak force. Once subjects were comfortable pushing at the low cadence, they gradually increased push frequency to help reduce peak force. Testing was completed for each subject when no further improvements in cadence, peak force and impact could be made. Across all subjects, the total number of trials ranged from 5 to 15, including the normal and education trials.

4.2.3 Data Analysis

Both left and right sides stroke-by-stroke values of contact angle, cadence, peak force and impact were averaged across all strokes within each trial. Three trials were selected from each subject: the normal trial, the education (EDU) trial, and the best multi-variable biofeedback (BMB) trial. All trial results for a subject were shown in Table 4.2. The BMB trial was the trial that resulted in the largest combined decrease in cadence, peak force, and impact. Trail 5 in table 4.2 was selected to be the BMB trial. To be considered for the BMB trial, all three values had to decrease by at least 5%. If a subject was unable to achieve these improvements, the requirements were loosened to include all trials in which cadence, peak force and impact decreased by any percentage. If no trials met these requirements, all trials were considered.

Once the BMB trial was selected for each subject, the average values of contact angle, cadence, peak force and impact were compared with the averages from the normal trial and the EDU trial. Results were normalized within subject by computing the relative change (%) in each variable. Percent changes were then averaged across subjects to determine the overall effect of each training component (EDU and BMB) and the relative differences between the two components. Paired t-tests were used to determine the significance of each percent change. To account for the 12 individual comparisons, alpha was adjusted to .004. The slope R1 and R2 values for each regression were determined in Matlab.

Table 4.2 All trial results for a subject

Trails					Percent different compare to normal trail			
	Cadence (push/min)	Peak force (N)	Contact angle (deg)	Impact (N/Sec)	Cadence	Peak force	Contact angle	Impact
NOR	75.1	94.8	79.1	1762	0	0	0	0
EDU	45.9	101.8	98.6	1269	-38.9	7.5	24.6	-28.0
1	57.7	111.3	94.9	1765	-23.1	17.5	19.9	0.2
2	59.8	99.1	89.4	1797	-20.3	4.6	13.0	2.0
3	67.8	90.5	82.5	1706	-9.7	-4.5	4.3	-3.2
4	65.2	93.0	84.8	1666	-13.1	-1.8	7.1	-5.5
5	63.2	82.9	92.9	1400	-15.8	-12.5	17.4	-20.6
6	71.2	75.8	90.5	1309	-5.1	-20.0	14.4	-25.7
7	71.4	77.9	93.6	1227	-4.8	-17.7	18.2	-30.4

4.3 Results

4.3.1 Participants

Thirty-two manual wheelchair users (30 men, 2 women) participated in this study. Twenty-four subjects had paraplegia (T3-L3), 5 had spina bifida (T10-L5), 1 had sacral agenesis, 1 had transverse myelitis, and 1 had a spinal lipoma. Subjects were (mean \pm SD) 37.6 ± 10.8 years old, weighed 78.9 ± 16.7 kg, and had 17.4 ± 11.2 years of manual wheelchair experience. Table 4.3 shows the mean handrim biomechanics for the normal propulsion trial.

Table 4.3 Mean \pm SD Handrim Biomechanics During Normal Treadmill Propulsion

Variable	Value
Speed (m/s)	1.32 ± 0.01
Power output (W)	10.98 ± 3.65
Braking moment (Nm)	0.86 ± 0.41
Contact angle (degrees)	92.70 ± 16.70
Cadence (strokes/minute)	57.39 ± 12.82
Peak force (N)	65.42 ± 22.21
Push distance (m)	1.47 ± 0.39
Impact (N/s)	1157.46 ± 482.27
Smoothness	0.69 ± 0.05

4.3.2 Effects of Education and Multivariable Biofeedback

The observed changes compared to normal trial in contact angle, cadence, peak force and impact for each training component are shown in Table 4.4. After viewing the education video, subjects responded by increasing contact angle

16%, decreasing cadence 19% and decreasing impact 16%; however, they also increased peak force over 10%. In 4 subjects, peak force increased more than 40%. When using the multivariable biofeedback display, subjects were able to decrease cadence (-13%), peak force (-10%) and impact (-24%) with an above average contact angle (12% larger). It took subjects 4.88 ± 2.58 trials to produce their BMB trial. Compared to the EDU trial, the BMB trial contact angle was 3.3% lower and cadence was 9.5% higher. On the other hand, the values of peak force and impact in the BMB trial were the lowest of any condition. Every subject was able to reduce cadence and impact while using the multivariable biofeedback, and all but one subject were able to reduce peak force. All percent changes were found to be significant ($p < .004$) except for the decrease in contact angle ($p = .045$) and the increase in cadence ($p = .004$) between the EDU and BMB trials.

Table 4.4 Percent Changes in Outcome Variables Compared to Normal Trial

Component	Contact Angle	Cadence	Peak Force	Impact
EDU	$16.6 \pm 14.2^*$	$-19.4 \pm 12.5^*$	$11.3 \pm 19.0^*$	$-16.6 \pm 18.0^*$
BMB	$11.9 \pm 10.4^*$	$-12.9 \pm 8.2^*$	$-10.1 \pm 6.7^*$	$-24.7 \pm 15.9^*$

Values are mean \pm SD and range, $*p < 0.04$. EDU=education trail; BMB=best multi-variable biofeedback trail.

The regression analysis revealed opposite trends in the changes in peak force and contact angle for the EDU and BMB trials (Figure 4.4). Peak force tended to increase with contact angle in the EDU trial and decrease with contact angle in the BMB trial. The R^2 values for both regressions were low ($R^2 < 0.04$),

although the trend lines demonstrate the difference in the relationships between changes in peak force and contact angle.

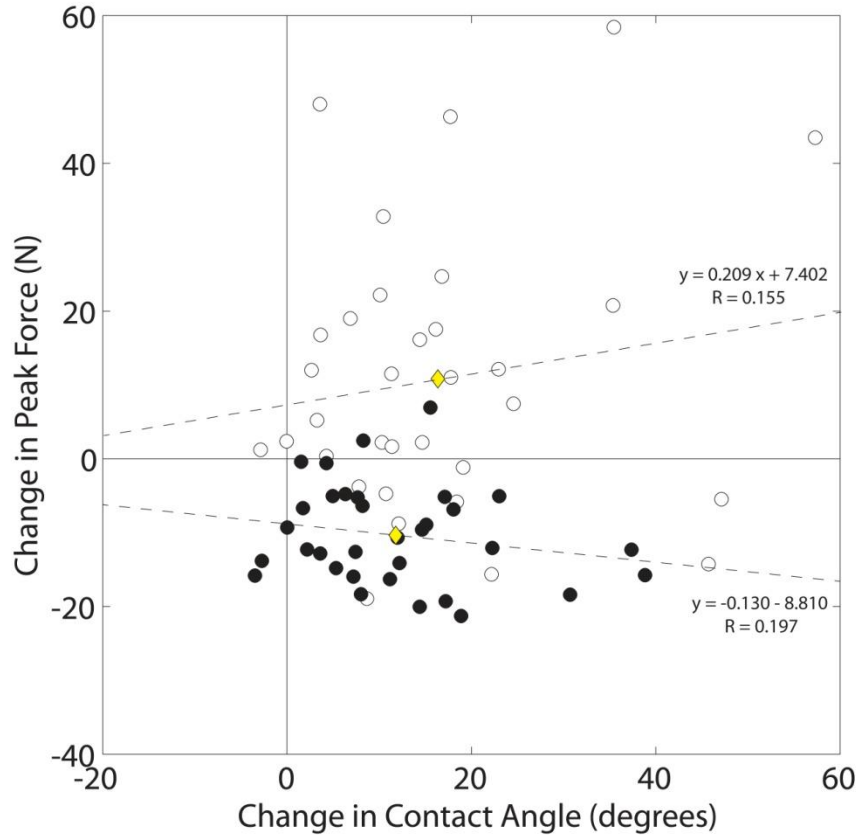


Figure 4.4 Trends in percent changes in peak force versus percent changes in contact angle for each training component; where \circ = EDU and \bullet = BMB. The diamonds indicate the mean data point for each component.

4.4 Discussion

The results of this study demonstrate the potential for experienced wheelchair users to make significant improvements in handrim biomechanics with the use of multivariable biofeedback. Reductions in cadence, peak force and impact were achieved by improving the length and direction of force application

on the handrim. The other critical component was the use of real-time force feedback. By monitoring continuous force profiles, subjects were able to avoid the increases in peak force that tend to occur when contact angle is increased[21]. Not only did subjects avoid increasing peak force, many decreased peak force by as much as 21%. The decrease was associated with a more moderate increase in contact angle and a smaller decrease in cadence.

The multivariable biofeedback used in this study was unique in that it featured a continuous plot of force versus contact angle and included target lines for each variable. From this interface, users can interpret at what wheel angle or at which position on the handrim the peak push force is reached and, if necessary, the amount of change needed to keep peak force below the maximum force line. At the same time, contact angle was evident by the length of the force profile or the number of vertical bars. The vertical target line reminded subjects to extend force application beyond their typical contact angle. The goal of this study is reducing peak force and cadence concurrently. The Multivariable biofeedback translated this goal to a simple way which is pushing below and beyond the two target lines. All these features of the multivariable biofeedback allow users to interpret the reinforcement (feedback) without too much focus.

Previous multivariable biofeedback displays have consisted of either a plot-table combination[21] or a discontinuous series of bar graphs[37], both of which seem to complicate the process of propulsion training. DeGroot et al. [21] used the SmartWheel Data Viewer to provide real-time feedback to subjects. The

Data Viewer includes plots of speed and tangential force along with a numeric display of time, speed and distance, and a table of current push values. The display was intended to be viewed by clinicians, who can follow specific variables of interest, not by users who may be overwhelmed by the amount of information on screen. The inability of subjects to reduce their peak force using the Data Viewer may be attributed to the complexity of the display. On the other hand, the biofeedback display developed by Rice et al.[37] was designed to maximize learning, focus, and transfer of motor skills. The biofeedback featured a discontinuous display of bar graphs of speed, contact angle and cadence. Although the display was consistent with motor learning theory, it would at times display all three bar graphs at once. The approach may have benefitted from consolidating contact angle and cadence and including force feedback, which may have helped reduce peak force.

Despite the overall success, the multivariable biofeedback training did not help every subject improve. It is important to remember that these results do not reflect the quality of each subject's propulsion technique, just their ability to improve. Some subjects began the study with excellent technique and admirable handrim biomechanics. Table 4.5 shows the data for 3 example subjects. Both subject 1 and subject 2 achieved small amount of combined reduction in cadence, peak force and impact. Subject 1 had an excellent propulsion technique with low peak force and low impact compared to other subjects, for example, subject 3. So subject 1 was not able to improve with the multivariable biofeedback.

Compared to others, subject 2 had a large contact angle and was not able to improve with the biofeedback.

The multivariable biofeedback provided to subjects was calculated with only one side wheel data and two sides of wheel data were processed in this study. Results showed that biofeedback could improve subject's propulsion technique for both hands. It may be not necessary for taking both side wheel data in the future study.

Table 4.5 Data for 3 example subjects

	Contact Angle	Cadence	Peak Force	Impact
Normal Trial Averages				
Subject 1	71.01	72.68	36.91	504.45
Subject 2	129.50	49.37	40.64	577.20
Subject 3	72.63	56.55	91.92	2372.57
% Change from Normal				
Subject 1	15.56	-13.42	6.94	-2.62
Subject 2	-3.49	-12.20	-15.82	-43.35
Subject 3	30.70	-30.39	-18.39	-52.19

4.5 Conclusion

Multivariable biofeedback provided by OptiPush is an effective method of generating improvements in manual wheelchair handrim biomechanics. By showing stroke-by-stroke force profiles, subjects were able to know when the max force occur and decrease peak force, cadence and impact while increasing contact angle. Based on CPG recommendations, all these improvements will reduce the possibility of UE pain and injury of manual wheelchair users.

CHAPTER V

CONCLUSION AND FUTURE DIRECTIONS

5.1 Project summary

In this project, the OptiPush Biofeedback System was designed, implemented, validated and tested. Physically, the system provides simple installation on most wheelchairs for a variety of wheel sizes. Functionally, the system provides acceptable accuracy and low error in measurements of wheel angle, speed, and handrim loading (in both static and dynamic conditions). The system calculates several variables that related to propulsion technique and provides this information to users as a real-time biofeedback. Testing of the biofeedback revealed a viable means of improving propulsion technique. Participants were able to make significant and controlled changes to both single and multi-variables biofeedback.

5.2 System application

The OptiPush biofeedback system is not only a wheelchair propulsion measurement device but also acts as a training tool that can improve wheelchair propulsion technique. Besides the work done by this project, the system is also well used by several other studies.

- 1) The system was used to compare the difference between pushing over-ground and on treadmill[38]. Most of the variables were nearly identical across the conditions and none of the differences were found to be statistically significant (Table 5.1).

Table 5.1 Comparison of propulsion variables between overground and treadmill

<i>Test Variable</i>	<i>Difference</i>			<i>P-</i> <i>value</i>
	<i>Overground</i>	<i>Treadmill</i>	<i>(%)</i>	
Speed (m/s)	1.10 (0.23)	1.10 (0.23)	-0.1	0.583
Cadence (push/min)	49.65 (10.92)	52.06 (10.83)	3.6	0.111
Average force (N)	38.9 (7.59)	38.9 (8.60)	-0.1	0.959
Contact Angle (deg)	87.49 (19.1)	87.48 (18.21)	-0.5	0.803
Power Out (w)	8.28 (2.26)	8.58 (2.53)	3.5	0.132
Peak Force (N)	57.46 (10.84)	57.22 (12.44)	0.4	0.853
Peak Torque (Nm)	10.81 (2.38)	10.76 (2.99)	1.6	0.460

Values are mean (s.d.).

- 2) The system was synchronized with other devices (motion capture, EMG) and all data was used to study wheelchair propulsion kinetically and dynamically. A PH.D student, Jeffery Wade Rankin, built an upper extremity musculoskeletal model based on these data and he received his PH.D degree at the University of Texas at Austin[39] (Figure 5.1).

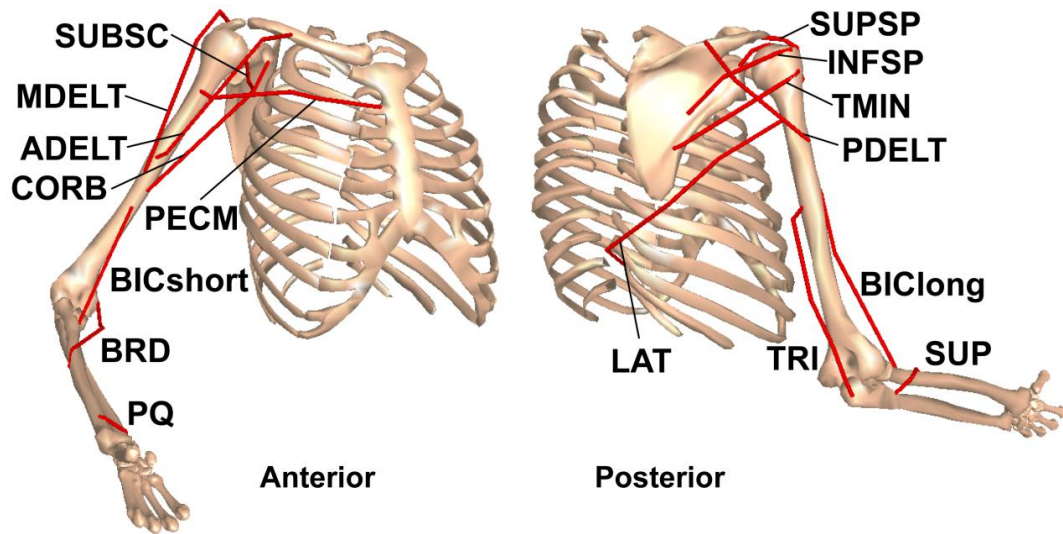


Figure 5.1 Musculoskeletal model used in the wheelchair propulsion simulations.

- 3) The effects of four different stroke pattern (Figure 5.2) were compared[40]. OptiPush system was used to measure Cadence, Peak Force, Contact Angle, Braking Torque and Impact with different stroke pattern. Results showed that Double Loop and Semi-Circular generated the best combinations of handrim biomechanics.

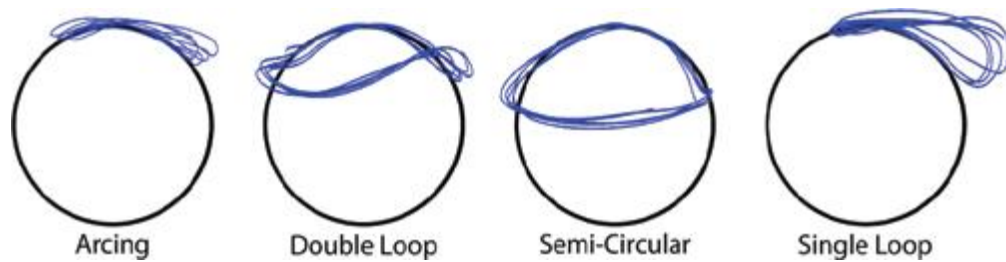


Figure 5.2 The four classified stroke patterns

- 4) Besides our lab, some other researchers used OptiPush biofeedback system in their studies (Table 5.2).

Table 5.2 Users of OptiPush Biofeedback System

Product Serial Number	Date of Purchase	Customers
PRO00001	Dec-2008	MAX Mobility, Antioch, TN, USA
PRO00002	Dec-2008	VA Palo Alto Health Care System, CA, USA
PRO00003	Dec-2008	VA Palo Alto Health Care System, CA, USA
PRO00004	Mar-2009	Biomechanics Lab, University of Extremadura, Spain
PRO00005	May-2010	Lucas Vander Woude group, University of Groningen, Netherland
PRO00006	May-2010	Lucas Vander Woude group, University of Groningen, Netherland
PRO00008	Jan-12	Lucas Vander Woude group, University of Groningen, Netherland

5.3 Future Directions

In order to get better performance, this project could be continued in the following areas:

- 1) The OptiPush Wheel measures three-dimensional forces and torques on the handrim using a commercially-available 6 DOF load cell (Delta,

ATI Industrial Automation, Apex, NC, USA). This load cell is the most expensive part compared to others in this system. A strain gauge system may be used to reduce price and total weight (Figure 5.3).

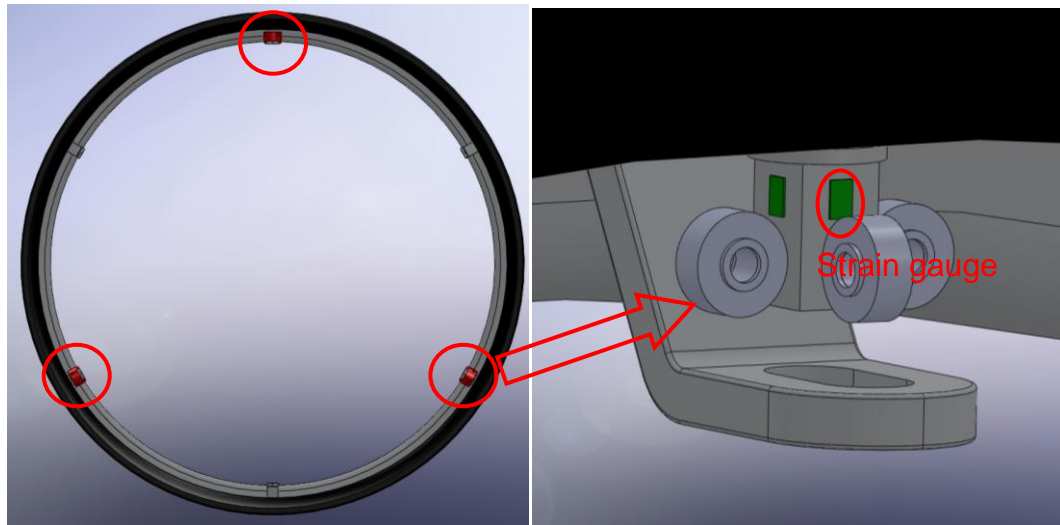


Figure 5.3 New strain gauge CAD design

- 2) A rotary absolute magnetic shaft encoder (MA3, US Digital, Vancouver, WA, USA) is used to measure the wheel angle (Figure 2.3). The encoder reports the shaft position over 360° with no stops or gaps. It has an analog voltage output of 0-5V that is proportional to absolute shaft position. This encoder has a non-linearity near 0V and 5V output (Figure 5.4). An Optical encoder without dead zone may be used for wheel angle measurement.

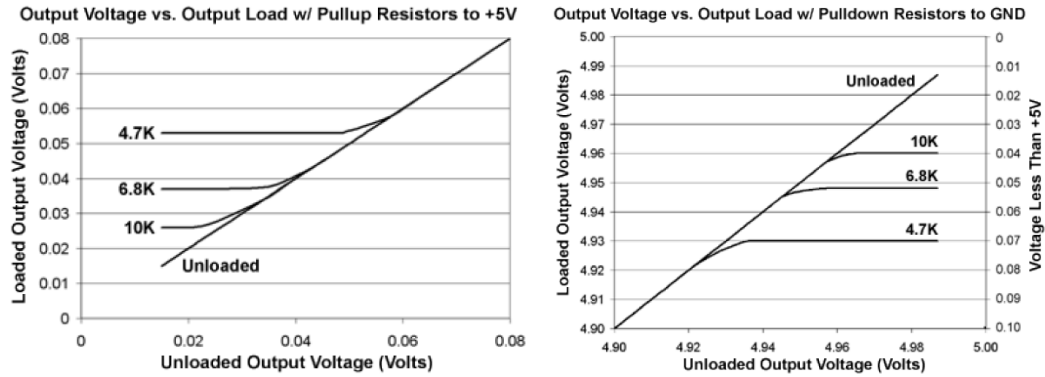


Figure 5.4 The non-linearity near 0V and 5V output

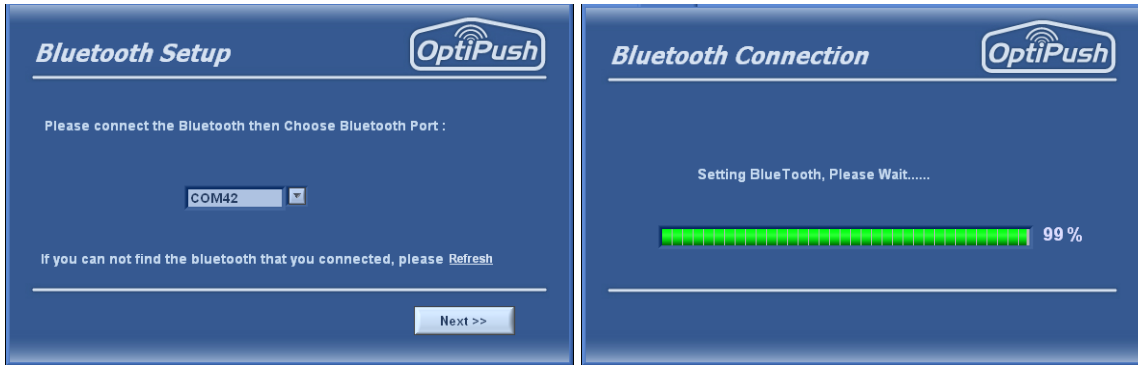
- 3) The OptiPush biofeedback system software uses LabView as environment. It requires a high end PC to run smoothly. In order to reduce the requirement, a microcontroller unit (MCU) could be used on the OptiPush instrumented wheel. The MCU will calculate all variables and transmit all results to a PC or a mobile device.
- 4) All the biofeedback testing was designed to study short term effects of biofeedback training. A longitudinal investigation could be done in the future to better understand the effects of biofeedback training over time with individual wheelchair users as it relates to injury developments.

5.4 Conclusion

This project successfully developed the instrumentation and software necessary to provide wheelchair users with real-time biofeedback on their propulsion stroke. The structure of the biofeedback was tested and refined in a series of human subject trials. The user testing revealed that propulsion technique could be altered and controlled with the use of biofeedback. It was also learned that there were competing interests between reducing push cadence and

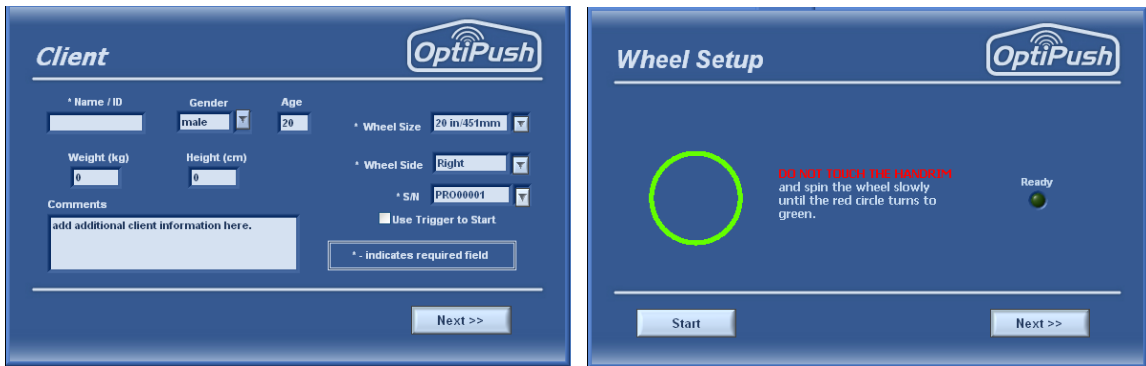
reducing peak handrim force. Repetitive stress injuries are likely influenced by either the magnitude of the joint loading, the repetition of the joint loading, or both. Because the exact etiology of overuse injuries in this population is not clear, it is ideal if both of these factors can be reduced. The final OptiPush biofeedback design included a multi-variable push stroke graph of peak force verses contact angle that was shown to enable the user to reduce both their peak handrim force and their push cadence concurrently. As a result of this accomplishment, researchers and clinicians around the globe will be able to implement this approach to further study its potential benefits on upper extremity health. It is hoped that the results of this project will have a lasting and positive effect on the quality of life of manual wheelchair users.

APPENDIX A: MAIN VI FRONT PANEL



(a)

(b)



(c)

(d)

Figure A-1 Interface of OptiPush software settings. (a) Bluetooth port selection; (b) Bluetooth connection; (c) Client information; (d) Wheel offset removal.

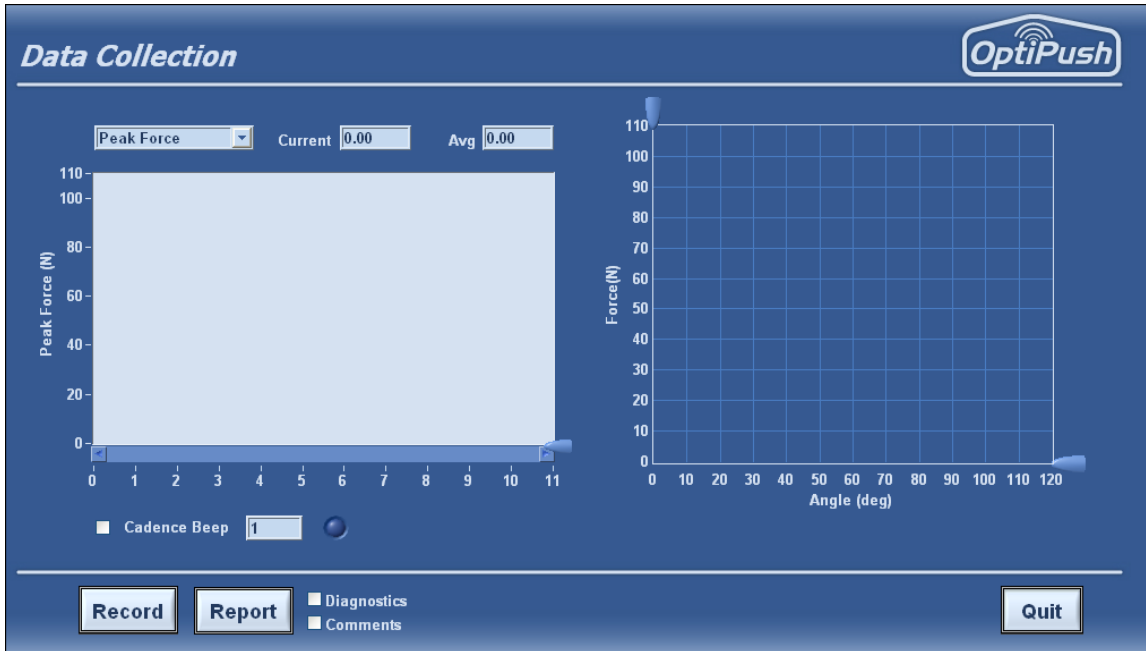


Figure A-2 Biofeedback interface of OptiPush software

APPENDIX B OPTIPUSH TESTING REPORT

OptiPush Test Report

Data & Time:	2/24/10 12:9
Description:	Propulsion Training --- Initial Visit

Client

Name:	John Smith
Gender:	male
Age:	25
Weight(kg):	78
Height(cm):	180
Wheel Size:	25 in/559mm
Wheel Side:	Right
Comment:	T-10 Para two years post injury

Results

Number of pushes:	22
Speed(m/s):	1.7
Cadence(push/min):	78
Braking Torque(Nm):	2.5
Distance(m):	1.3
Coast Time(s):	0.5
Peak Force(N):	83
Peak Torque(Nm):	20
Smoothness:	0.5
Contact Angle(deg):	71
Power(W):	17
Impact(N/s):	1542

Diagnostics

Speed slower than average (1.2 m/s)?	No
Peak force higher than average (68 N)?	Yes
Cadence higher than average (61 push/min)?	Yes

References :

[1] Richter VM, Rodrigues R, Woods KR, Axelson P W. Stroke Pattern and Handrim Biomechanics for Level and Uphill Wheelchair Propulsion at Self-Selected Speeds. Arch Phys Med Rehabil 2007;88:61-7.

[2] Cowan RE, Boninger ML, Sawatzky BJ, Mazoyer BD, Cooper RA. Preliminary Outcomes of the SmartWheel Users' Group Database : A Proposed Framework for Clinicians to Objectively. Arch Phys Med Rehabil 2008;89:260-8.



APPENDIX C TREADMILL VALIDATION

Spinal Cord (2010), 1–6
© 2010 International Spinal Cord Society All rights reserved. 1362-4393/10 \$32.00
www.nature.com/sc



ORIGINAL ARTICLE

Comparing handrim biomechanics for treadmill and overground wheelchair propulsion

AM Kwarciak, JT Turner, L Guo, WM Richter

Biomechanics Laboratory, MAX Mobility, LLC, Antioch, TN, USA

Study design: Cross-sectional study.

Objectives: To compare handrim biomechanics recorded during overground propulsion with those recorded during propulsion on a motor-driven treadmill.

Setting: Biomechanics laboratory.

Methods: In all, 28 manual wheelchair users propelled their own wheelchairs, at a self-selected speed, on a low-pile carpet and on a wheelchair accessible treadmill. Handrim biomechanics were recorded with an OptiPush instrumented wheelchair wheel.

Results: Across the two conditions, all handrim biomechanics were found to be similar and highly correlated ($r > 0.85$). Contact angle, peak force, average force and peak axle moment differed by 1.6% or less across the two conditions. Although not significant, power output and cadence tended to be slightly higher for the treadmill condition (3.5 and 3.6%, respectively), owing to limitations in adjusting the treadmill grade.

Conclusion: Based on the results of this study, a motor-driven treadmill can serve as a valid surrogate for overground studies of wheelchair propulsion.

Spinal Cord advance online publication, 2 November 2010; doi:10.1038/sc.2010.149

Keywords: wheelchair; biomechanics; propulsion; treadmill; handrim; kinetics

Introduction

Manual wheelchair users are at an increased risk of upper limb pain and pathology owing to the repetitive loads associated with wheelchair propulsion.^{1,2} For this reason, wheelchair propulsion continues to be the focus of a number of research studies.^{3–11} Although these studies share a common goal of helping to reduce the risk of injury to manual wheelchair users, the methods of reaching that goal vary, particularly with respect to the testing environment. In these studies, propulsion testing was conducted overground,^{3–5} on a dynamometer,^{6–8} or on a treadmill.^{9–11} Each of these testing environments offers its own advantage, though with the treadmill and the dynamometer, the edge comes at the cost of typical propulsion. Ideally, all studies of manual wheelchair propulsion would be conducted overground, as it represents the most realistic testing condition. However, overground data collection can be limiting. In order to capture a number of consecutive strokes, a sufficiently long distance is needed. This distance may not be available, or allowable, given the restrictions of the measurement equipment (motion capture, electromyogra-

phy, cardiopulmonary diagnostics, so on). With overground testing, it is also difficult to control experimental conditions such as velocity and power output.¹²

An alternative means of conducting studies of wheelchair propulsion is with a motor-driven treadmill. A treadmill provides a confined and consistent testing environment in which wheel velocity and power output can be controlled. The ability to control parameters that affect testing consistency makes the treadmill useful for studying the effects of propulsion training and other interventions.¹³ To appreciate the similarity of treadmill testing to overground testing, we must study the similarity of the testing results. The only comparative study involving the two conditions, conducted by Stephens and Endsberg,¹⁴ examined recovery patterns during propulsion overground, on a dynamometer and on a pair of treadmills. As most wheelchairs are too wide to fit on a traditional exercise treadmill, the treadmill condition was created by having subjects straddle two independent treadmills running at the same speed. Data from the dynamometer and dual-treadmill conditions were combined into a single condition, making it difficult to conclude what affects, if any, the dual treadmill had on recovery pattern.

The objective of this study was to compare handrim biomechanics recorded during overground propulsion (reference condition) with those recorded for the same subjects, with similar velocity and power output, during treadmill

Correspondence: AM Kwarciak, Biomechanics Laboratory, MAX Mobility, LLC, 5425 Mount View Parkway, Antioch, TN 37013, USA.
E-mail: andrew@max-mobility.com
Received 7 June 2010; revised 3 September 2010; accepted 28 September 2010

propulsion (experimental condition). We hypothesized that handrim biomechanics on a treadmill would be substantially equivalent to those found while pushing overground.

Materials and methods

Subjects

In all, 31 full-time manual wheelchair users, identified from an internal subject database and by local rehabilitation professionals, were recruited for this study. The criteria for participation included: use of a manual wheelchair as the primary mode of mobility, full function in the upper limbs with no debilitating pain, healthy enough to propel for 5 min at a time and the use of quick-release rear axles. Before enrollment, all subjects provided informed consent. All study documents and test procedures were approved by the Western Institutional Review Board (Olympia, WA, USA).

Instrumentation

Data for this study were collected with an OptiPush instrumented wheelchair wheel (MAX Mobility, LLC, Antioch, TN, USA). The OptiPush measures wheel angle and the three-dimensional forces and moments applied to the handrim during propulsion. Data are sampled at 200 Hz and transmitted via bluetooth to a laptop running the OptiPush software. The software filters forces and moments using a 4th order digital Butterworth filter with a low-pass cutoff frequency of 20 Hz.¹⁵ Filtered kinetics and wheel angle measurements are then used to compute propulsion variables on a stroke-by-stroke basis. Each push stroke (push and recovery phases) is defined by the absolute moment about the axle. The push phase begins when moment about the axle exceeds 1 Nm and the recovery phase begins when moment about the axle drops back within 1 Nm.

Data collection

Data for this study were obtained from a larger study of wheelchair propulsion. The methods listed here are limited to the procedures used to collect the data for this investigation.

The wheels of each subject's wheelchair were removed and replaced by the OptiPush wheel on the right (6.0 kg for a 0.64 m wheel) and an inertia-compensated wheel on the left.

The diameters of the wheels and handrims were chosen to match those used by the subject. Both wheels were fitted with a low-profile pneumatic tire inflated to 100 pounds per square inch. Once the wheels were attached and the OptiPush was initialized, subjects propelled their wheelchairs across a low-pile, commercial carpet with no pad (about 50 m long). Subjects were asked to select a speed that could be maintained for an extended period of time. This was done to help prevent fatigue during treadmill testing. Allowing subjects to propel at a self-selected speed also helped to prevent unwanted changes in normal propulsion technique, which may be affected by speed.¹⁶ Two separate runs were made across the floor, in opposite directions, to account for any surface irregularities. Data from the first 3–4 strokes of each trial (initial acceleration phase¹⁷) and the last 3–4 strokes (deceleration phase) were disregarded. Steady-state data from each trial were combined into a single matrix from which average overground speed, power output and the resulting handrim biomechanics were computed. Table 1 lists the equations for all variables assessed in this study.

Subjects were then loaded onto a wheelchair accessible treadmill (Figure 1). Unlike standard treadmills, this treadmill has a wide belt (1.06 m) and a dynamic safety system. The front of the wheelchair was strapped to the frame of the treadmill using two straps that ride along linear bearings. The straps keep the wheelchair on the treadmill and prevent



Figure 1 Photo of the treadmill test setup.

Table 1 Propulsion variables

Variable	Description (Units)	Equation
Speed	Mean speed during the stroke, (ms^{-1})	$(\theta_{\text{stroke}}/180) \cdot \pi \cdot D/t_{\text{stroke}}$
Cadence	Push frequency, (pushes min^{-1})	$60/t_{\text{stroke}}$
Contact angle	Angle through which wheel rotates when hand is on handrim, (degrees)	Wheel angle at recovery start – wheel angle at push start
Power output	Power generated per stroke, (Watts)	$\Sigma(M_{\text{axle}} \cdot \Delta\theta \cdot \pi/180)/t_{\text{stroke}}$
Peak force	Maximum total force applied to the handrim during the stroke, (Newtons)	$\text{Max}(F_{\text{tot}})$, where $F_{\text{tot}} = \sqrt{F_x^2 + F_y^2}$
Average force	Average total force applied to the handrim during the stroke, (Newtons)	Mean (F_{tot})
Peak moment	Maximum moment about the axle during the stroke, (Newton-meters)	Max (M_{axle})

Abbreviations: D , wheel diameter (m); θ , wheel angle (degrees); θ_{stroke} , angle through which the wheel rotates during the stroke (degrees); t_{stroke} , time to complete the stroke (s); $\Delta\theta$, point-to-point change in angle (degrees).

excessive lateral sway; however, they do not impede fore-aft movement of the wheelchair. Subjects were given several minutes to acclimate to pushing on the treadmill. During the acclimation period, the treadmill speed was set to match the subject's average overground speed and a metronome beep was provided to help the subject match treadmill cadence to overground cadence. The grade of the treadmill was increased until the subject's treadmill power output, measured on a stroke-by-stroke basis, matched the average overground power output (The average treadmill grade across all subjects was $0.81 \pm 0.28\%$). Once the acclimation period was complete, the treadmill was stopped and subjects were given time to rest. After a few minutes, the treadmill was re-started and subjects were asked to push their wheelchair for approximately 1 min while OptiPush data were recorded from the right side.

Data analysis

Seven propulsion variables, computed from data collected during the overground and treadmill trials, were compared across the two testing conditions (Table 1). These variables were selected because they are common in studies of wheelchair propulsion and have been related to upper limb health.^{1,2,18} For each subject, the variables were averaged across all strokes (minimum of 15 strokes) for each condition. Paired *t*-tests were used to analyze the differences between the mean treadmill value and the mean overground value for each variable, with the null hypothesis that the difference would equal zero. To maximize the sensitivity, no type I error correction was applied and α was set to 0.05. Pearson's product-moment correlation coefficients were also calculated to assess the relationship between the variables calculated from each condition. For visual confirmation, scatter plots of each variable (excluding speed) were created. The plots include a line of equality (slope of 1 and intercept of 0) to evaluate the similarity of the variables. The statistical power of the study was estimated to be 77%, based on an s.d. of 20% and a detectable change of 10%. All statistical analyses were performed using SPSS (SPSS Inc., Chicago, IL, USA) and all plots were made using MATLAB (The Math-Works, Inc., Natick, MA, USA).

We certify that all applicable institutional and governmental regulations concerning the ethical use of human volunteers were followed during the course of this research.

Results

Subjects

A complete set of data were obtained from 28 subjects (24 men, 4 women). Data from three individuals could not be used as the protocol was not followed correctly. This reduced the projected study power to 72%. The remaining subjects ranged in age from 15 to 57 years (34.2 ± 9.5 years) and in duration of injury from 2 to 43 years (14.5 ± 10.4 years). Of the 28 subjects, 20 had paraplegia (T3-L1), 5 had spina bifida (T10-L5), 1 had tetraplegia (C6-7 incomplete), 1 had cerebral palsy and 1 had a spinal lipoma.

Table 2 Comparison of propulsion variables for each condition

Test variable	Overground	Treadmill	Difference (%)	P-value
Speed ($m s^{-1}$)	1.09 (0.23)	1.09 (0.23)	-0.1	0.583
Power output (W)	8.43 (2.32)	8.72 (2.59)	3.5	0.132
Cadence (pushes min^{-1})	50.6 (10.9)	52.4 (11.1)	3.6	0.111
Contact angle (degrees)	86.6 (19.1)	86.2 (18.1)	-0.5	0.803
Peak force (N)	58.1 (11.1)	58.4 (12.4)	0.4	0.853
Average force (N)	38.9 (7.59)	38.9 (8.60)	-0.1	0.959
Peak moment (Nm)	10.9 (2.47)	11.0 (2.98)	1.6	0.460

Values are mean (s.d.).

Table 3 Pearson's correlation coefficients

Test Variable	r	P-value
Speed ($m s^{-1}$)	0.999	<0.001
Power output (W)	0.924	<0.001
Cadence (pushes min^{-1})	0.862	<0.001
Contact angle (deg)	0.883	<0.001
Peak force (N)	0.863	<0.001
Average force (N)	0.851	<0.001
Peak moment (Nm)	0.917	<0.001

Comparison of variables

Table 2 lists the variables calculated for each condition and the percentage differences between them. Most of the variables were nearly identical across the conditions with no greater than 1.6% difference between the averages. Furthermore, none of the differences were found to be statistically significant. Table 3 shows the results of the Pearson's correlation analysis. As expected, the analysis produced high *r*-values and low *P*-values indicating strong correlations between the variables in each condition. The proximity of the variables to each line of equality (Figure 2) also demonstrated the congruencies between the two sets of variables.

Discussion

The results of this study demonstrate the strong similarities in handrim biomechanics between treadmill and overground manual wheelchair propulsion. No statistically significant differences were found between the two conditions. This does not prove equivalence; however, it does not refute it. For this comparison, the most revealing results are the descriptive statistics. Four of the five uncontrolled variables calculated during treadmill propulsion (contact angle, peak force, average force and peak moment) were within 2% of the values recorded during overground propulsion. In addition, every variable was highly correlated between the two conditions ($r > 0.85$) and tightly distributed around the line of equality for the two testing environments (Figure 2).

Compared with previous studies of wheelchair propulsion on a treadmill,^{9,11} the power output measured in this study was 15–65% lower. The lower power output values are attributed to a slower belt speed and/or lesser treadmill

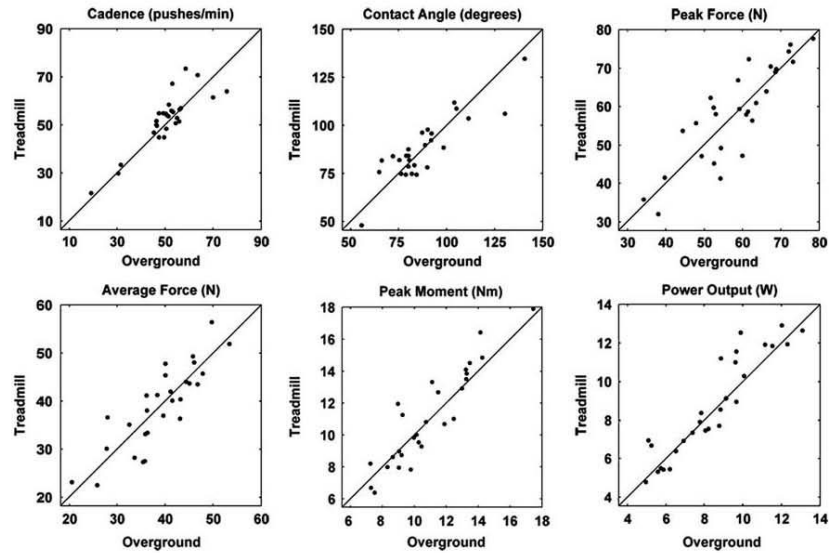


Figure 2 Plots of the variables (top row: cadence, contact angle and peak force; bottom row: average force, peak moment and power output). Each plot includes a line of equality ($y=x$) to show the proximity of the points to being equal across the treadmill and overground conditions.

grade. Given the lower power output values, it is reasonable that the values of contact angle and cadence measured in this study were also lower than in previous studies. On the other hand, average peak force (58.4 N) was within the range of reported values (53.5–58.9 N) for treadmill propulsion.^{9,11}

Although we found no significant differences between the propulsion variables, subtle differences were seen in power output, cadence and peak moment. Power output was a controlled variable that should have been equivalent across the two conditions. Power was adjusted by increasing treadmill grade, which ranged from 0.4° to 1.7° for all subjects, until the power output measured by the OptiPush was similar to the mean power output of the overground trials. The resolution for adjusting grade was 0.1°, which limited our ability to fine tune power output on the treadmill. With greater control over treadmill grade, we are confident that power output could have been adjusted to match the overground condition.

During treadmill propulsion, cadence and peak moment were 3.6 (1.8 pushes min⁻¹) and 1.6% (0.17 Nm) higher, respectively, than during overground propulsion. The increases in both variables were likely due to the increased power output requirement of the treadmill. On average, subjects did not increase their contact angle (-0.5%) or average force (-0.1%), and made a marginal increase in peak force (0.4%). Therefore, to achieve the higher power output on the treadmill, subjects increased their strokes per minute and, to a lesser extent, the peak moment of each stroke. Although the data support this conclusion, we cannot rule

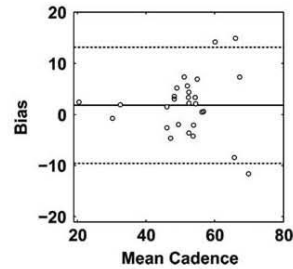


Figure 3 Bland-Altman plot of cadence. The solid line represents the mean difference in cadence between pushing on a treadmill and pushing overground, and the dashed lines define the 95% confidence interval.

out the possibility that subjects altered their technique, particularly cadence, in response to pushing on a treadmill. To help subjects become comfortable on the treadmill we had them push for 2–3 min before data collection. We believe this is an important step, as most wheelchair users have never pushed on a treadmill. Additional time may have helped subjects settle into a lower cadence; however, the acclimation period was purposely limited to avoid subject fatigue.

A supplementary Bland-Altman plot of cadence (Figure 3) was created to further investigate the changes in push frequency. The plot shows a slight trend in the differences between overground and treadmill cadence. Subjects who

pushed more frequently experienced greater changes in cadence across the two conditions. However, given the relatively few number of data points at the extremes, it is difficult to determine whether there is a definitive trend or whether these subjects are outliers. The majority of the subjects pushed at a rate of about 50 strokes min⁻¹. Within this group, there was an even distribution of bias with no apparent trend. The only clear result demonstrated by the plot is a small bias (mean offset from zero) when pushing on the treadmill.

From a mechanics perspective, the two testing conditions should produce similar results. van Ingen Schenau¹⁹ provides an analysis of bipedal locomotion on both treadmill and overground. Assuming that treadmill belt speed remains constant and air resistance is negligible, treadmill locomotion is mechanically similar to overground locomotion. The same should hold true for wheelchair propulsion. The external forces acting on a wheelchair user (gravity and ground reaction force) are the same as those acting on a bipedal walker. By selecting a coordinate system that moves with the belt,¹⁹ wheelchair propulsion on a treadmill can be described with the same model used to describe overground wheelchair propulsion.²⁰

Along with biomechanics, one must consider the advantages and disadvantages of treadmill use. In addition to providing control over speed and power output, treadmills provide the means to study steady-state activity in a limited space. This makes it easier to acquire data from motion capture systems and any tethered or cumbersome devices (for example, a cardiopulmonary monitor). Treadmills also provide unobstructed, pure pushing environments that can be used to develop upper body endurance, as well as proper muscle memory and biomechanics. In this way, treadmills are beneficial to rehabilitation clinics and fitness centers that provide propulsion training and exercise services. On the other hand, treadmills can be expensive, costing over \$10 000. Also, the treadmill cannot adequately represent the changes in surface, speed and direction that occur during typical wheeling. Overground testing represents the most realistic environment for studies of wheelchair propulsion. However, based on the similarities in mechanics and the variables computed in this study, the motor-driven treadmill provides an acceptable substitute when space is limited or when steady-state propulsion is desired. Researchers and clinicians can use these data to support their own use of treadmill testing.

There were several limitations to this study. First, upper body kinematics during overground and treadmill propulsion were not collected, so we could not determine whether there were differences in joint ranges of motion between the conditions. However, based on the strong similarities between the contact angle for the two conditions and the kinematic constraints on the upper extremity during the push, this seems unlikely. And second, we only studied a single power output level. Future work should include additional power output levels, as well as kinematics, metabolics and electromyography to provide a more comprehensive validation of treadmill use for studying wheelchair propulsion.

Conclusions

The motor-driven treadmill provides a controlled environment that is suitable for studying manual wheelchair propulsion. Subjects demonstrated similar handrim biomechanics to those measured during overground propulsion. The values of each propulsion variable were similar and highly correlated across the two testing conditions. To maintain comparable conditions to those overground, proper adjustments must be made to the treadmill to replicate overground speed and power output. Adequate time should also be given to help wheelchair users get accustomed to pushing on a moving belt. With these provisions, the treadmill provides a valid method of measuring wheelchair handrim biomechanics and may be an acceptable surrogate for overground studies when a controlled propulsion environment is desired.

Conflict of interest

We confirm that we have a financial interest in the subject matter and materials discussed in this paper. The authors are all employed by MAX Mobility, LLC, which currently offers a wheelchair-accessible treadmill. By demonstrating the similarity of treadmill propulsion to overground propulsion, we could gain from the potential increase in treadmill sales.

Acknowledgements

We would like to thank Russell Rodriguez for his help with subject recruitment, hardware setup, and data collection. This study was funded by the National Institutes of Health (1 R01 HD053732-01).

References

- Boninger ML, Cooper RA, Baldwin MA, Shimada SD, Koontz AM. Wheelchair pushrim kinetics: body weight and median nerve function. *Arch Phys Med Rehab* 1999; 80: 910–915.
- Mercer JL, Boninger M, Koontz A, Ren D, Dyson-Hudson T. Shoulder joint kinetics and pathology in manual wheelchair users. *Clin Biomech (Bristol, Avon)* 2006; 21: 781–789.
- Desroches G, Dumas R, Pradon D, Vaslin P, Lepoutre FX, Cheze L. Upper limb joint dynamics during manual wheelchair propulsion. *Clin Biomech (Bristol, Avon)* 2010; 25: 299–306.
- Koontz AM, Roche BM, Collinger JL, Cooper RA, Boninger ML. Manual wheelchair propulsion patterns on natural surfaces during start-up propulsion. *Arch Phys Med Rehabil* 2009; 90: 1916–1923.
- Cowan RE, Nash MS, Collinger JL, Koontz AM, Boninger ML. Impact of surface type, wheelchair weight, and axle position on wheelchair propulsion by novice older adults. *Arch Phys Med Rehabil* 2009; 90: 1076–1083.
- Rice J, Gagnon D, Gallagher J, Boninger M. Hand rim wheelchair propulsion training using biomechanical real-time visual feedback based on motor learning theory principles. *J Spinal Cord Med* 2010; 33: 33–42.
- DeGroot KK, Hollingsworth HH, Morgan KA, Morris CL, Gray DB. The influence of verbal training and visual feedback on manual wheelchair. *Disabil Rehabil Assist Technol* 2009; 4: 86–94.
- Lighthall-Haubert L, Requejo PS, Mulroy SJ, Newsam CJ, Bontrager E, Gronley JK et al. Comparison of shoulder muscle electromyographic activity during standard manual wheelchair

- and push-rim activated power assisted wheelchair propulsion in persons with complete tetraplegia. *Arch Phys Med Rehabil* 2009; 90: 1904–1915.
- 9 Gil-Agudo A, Ama-Espinosa A, Perez-Rizo E, Perez-Nombela S, Crespo-Ruiz B. Shoulder joint kinetics during wheelchair propulsion on a treadmill at two different speeds in spinal cord injury patients. *Spinal Cord* 2010; 48: 290–296.
 - 10 Bregman DJ, Drongelen SV, Veeger HE. Is effective force application in handrim wheelchair propulsion also efficient? *Clin Biomech (Bristol, Avon)* 2009; 24: 13–19.
 - 11 Richter WM, Rodriguez R, Woods KR, Axelson PW. Stroke pattern and handrim biomechanics for level and uphill wheelchair propulsion at self-selected speeds. *Arch Phys Med Rehabil* 2007; 88: 81–87.
 - 12 Van der Woude LH, Veeger HE, Dallmeijer AJ, Janssen TWJ, Rozendaal LA. Biomechanics and physiology in active manual wheelchair propulsion. *Med Eng Phys* 2001; 23: 713–733.
 - 13 Haisma JA, Van der Woude LH, Stam HJ, Bergen MP, Sluis TA, Bussmann JB. Physical capacity in wheelchair-dependent persons with a spinal cord injury: a critical review of the literature. *Spinal Cord* 2006; 44: 642–652.
 - 14 Stephens CL, Engsborg JR. Comparison of overground and treadmill propulsion patterns of manual wheelchair users with tetraplegia. *Disabil Rehabil Assist Technol* 2010; 5: 420–427.
 - 15 Cooper RA, DiGiovine CP, Boninger ML, Shimada SD, Robertson RN. Frequency Analysis of 3-Dimensional Pushrim Forces and Moments for Manual Wheelchair Propulsion. *Automedica* 1998; 16: 355–365.
 - 16 De Groot S, Veeger HE, Hollander AP, Van der Woude LH. Effect of wheelchair stroke pattern on mechanical efficiency. *Am J Phys Med Rehabil* 2004; 83: 640–649.
 - 17 Koontz AM, Cooper RA, Boninger ML, Yang Y, Impink BG, Van der Woude LH. A kinetic analysis of manual wheelchair propulsion during start-up on select indoor and outdoor surfaces. *J Rehabil Res Dev* 2005; 42: 447–458.
 - 18 Preserving Upper Limb Function in Spinal Cord Injury. *A Clinical Practice Guideline for Health-Care Professionals*. Consortium for Spinal Cord Medicine. Spinal Cord Medicine, Clinical Practice Guideline: Washington, DC, 2005.
 - 19 van Ingen Schenau GJ. Some fundamental aspects of the biomechanics of overground versus treadmill locomotion. *Med Sci Sports Exer* 1980; 12: 257–261.
 - 20 Cooper RA. A systems approach to the modeling of racing wheelchair propulsion. *J Rehab Res Dev* 1990; 27: 151–162.

REFERENCE LIST

1. IH Sie, RL Waters, RH Adkins, and H Gellman (1992): Upper extremity pain in the postrehabilitation spinal cord injured patient. *Arch Phys Med Rehab* 73:44.
2. Cooper, R. A., Boninger, M. L., Shimada, S. D., O'Connor, T. J., and DiGiovine, C. P. Manual wheelchair user upper extremity pain. 1996.
3. MM Rodgers and MA Finley (2002): Wheelchair propulsion biomechanics with upper extremity impairment and fatigue. *Proceedings of the 2002 World Congress of Biomechanics*
4. AM Koontz, ML Boninger, J Towers, RA Cooper, and M Baldwin (1999): Propulsion forces and MRI evidence of shoulder impairment. *Proceedings of the American Society of Biomechanics 1999 Annual Meeting* 296.
5. LH Van der Woude, G de Groot, AP Hollander, GJ van Ingen Schenau, and RH Rozendal (1986): Wheelchair ergonomics and physiological testing of prototypes. *Ergonomics* 29:1561.
6. R Niesing, F Eijskoot, R Kranse, AH den Ouden, J Storm, HEJ Veeger, LHV van der Woude, and CJ Snijders (1990): Computer-controlled wheelchair ergometer. *Med.Biol.Eng.Comput.* 28:329.
7. S De Groot, HE Veeger, AP Hollander, and LH Van der Woude (2005): Influence of task complexity on mechanical efficiency and propulsion technique during learning of hand rim wheelchair propulsion. *Med Eng Phys* 27:41.

8. HW Wu, LJ Berglund, FC Su, B Yu, A Westreich, KJ Kim, and KN An (1998): An instrumented wheel for kinetic analysis of wheelchair propulsion. *J Biomech Engr* 120:533.
9. MB Sabick, BR Kotajarvi, and KN An (2004): A new method to quantify demand on the upper extremity during manual wheelchair propulsion. *Arch Phys Med Rehabil* 85:1151.
10. KT Asato, RA Cooper, RN Robertson, and JF Ster (1993): SMARTWheels: development and testing of a system for measuring manual wheelchair propulsion dynamics. *IEEE Transactions on Biomedical Engineering* 40:1320.
11. RA Cooper, J Ster, III, and T Heil (1991): Development of a New ISO Wheelchair Two-Drum Tester. *Annual International Conference of the IEEE Engineering in Medicine and Biology Society* 13:1867.
12. Cooper, R. A., Asato, K. T., Robertson, R. N., and Ster, J. F. 2-Dimensional kinetic analysis of manual wheelchair propulsion with an improved SMARTwheel. 14, 1544-1545. 1992. Paris, France. 14th Annual IEEE/EMBS International Conference.
13. I Rice, B Impink, C Niyonkuru, and M Boninger (2008): Manual wheelchair stroke characteristics during an extended period of propulsion. *Spinal Cord*.
14. WJ Hurd, MM Morrow, KR Kaufman, and KN An (2008): Wheelchair propulsion demands during outdoor community ambulation. *J.Electromyogr.Kinesiol*.

15. RE Cowan, ML Boninger, BJ Sawatzky, BD Mazoyer, and RA Cooper (2008): Preliminary outcomes of the SmartWheel Users' Group database: a proposed framework for clinicians to objectively evaluate manual wheelchair propulsion. *Arch.Phys.Med.Rehabil.* 89:260.
16. R Rodriguez, WM Richter, KR Woods, and PW Axelson (2004): Reducing variability in wheelchair propulsion outcomes. RESNA 27th International Annual Conference
17. WM Richter, R Rodriguez, KR Woods, and PW Axelson (2006): Stroke pattern and handrim biomechanics for level and uphill wheelchair propulsion at self-selected speeds. *Arch Phys Med Rehab* 88:81.
18. MJ Dvorznak, RA Cooper, TJ O'Connor, and ML Boninger (1997): Braking Study. *Rehab R&D Prog Rpts* 294.
19. S De Groot, HE Veeger, AP Hollander, and LH Van der Woude (2002): Consequence of feedback-based learning of an effective hand rim wheelchair force production on mechanical efficiency. *Clin Biomech* 17:219.
20. BR Kotajarvi, JR Basford, KN An, DA Morrow, and KR Kaufman (2006): The effect of visual biofeedback on the propulsion effectiveness of experienced wheelchair users. *Arch Phys Med Rehabil* 87:510.
21. K DeGroot, H Hollingsworth, Morgan K, orris CL, and D ray (2009): The influence of verbal training and visual feedback on manual wheelchair. *Disabil.Rehabil.Assist.Technol.* 4:86.

22. ML Boninger, AM Koontz, SA Sisto, TA Dyson-Hudson, M Chang, R Price, and RA Cooper (2005): Pushrim biomechanics and injury prevention in spinal cord injury: Recommendations based on CULP-SCI investigations. *J Rehabil Res Dev.* 42:9.
23. KR Woods, WM Richter, R Rodriguez, and PW Axelson (2004): Removal of dynamic offset signal from load cell instrumented wheels. RESNA 27th International Annual Conference
24. ML Boninger, RA Cooper, MA Baldwin, SD Shimada, and AM Koontz (1999): Wheelchair pushrim kinetics: body weight and median nerve function. *Arch Phys Med Rehab* 80:910.
25. WM Richter, TJ O'Connor, DA Chesney, PW Axelson, ML Boninger, and RA Cooper (2000): Effect of pushrim compliance on propulsion efficiency. *Proceedings of the RESNA 2000 Annual Conference* 381.
26. LH Van der Woude, HE Veeger, RH Rozendal, and AJ Sargeant (1989): Optimum cycle frequencies in hand-rim wheelchair propulsion. *Wheelchair propulsion technique. Eur J Appl Physiol Occup Physiol* 58:625.
27. Skinner BF: *Science and Human Behavior*. New York, Macmillan, 1953.
28. Mark Stephen Schwartz, Frank Andrasik: *Biofeedback: a practitioner's guide*, 2003.
29. Ronald V. Croce, *The effects of EMG biofeedback on strength acquisition. Applied Psychophysiology and Biofeedback*, Volume 11, Number 4, 299-310.

30. Ken Ohta, et al. Miyaji. Dynamics-based Force Sensor Using Accelerometers-application of Hammer Throw Training Aid. *The Engineering of Sport*, 2008, 207-213.
31. A. Barney Alexander, et al. A Comparison of Auditory and Visual Feedback in Biofeedback Assisted Muscular Relaxation Training. *Psychophysiology*, 1975 Mar;12(2):119-23.
32. B. Peacock, et al. Feedback and maximum voluntary contraction. *Ergonomics*, 1981, 24(3): 223-228.
33. Levitt, R., Deisinger, J. A., Wall, J. R., Ford, L., & Cassisi, J. E. EMG feedback-assisted postoperative rehabilitation of minor arthroscopic knee surgeries. *The Journal of Sports Medicine and Physical Fitness*, (1995). 35, 218–223.
34. Steven L. Cohen. Et al. EMG Biofeedback: The Effects of CRF, FR, VR, FI, and VI Schedules of Reinforcement on the Acquisition and Extinction of Increases in Forearm Muscle Tension. *Applied Psychophysiology and Biofeedback*, Vol. 26, No. 3, 2001
35. Consortium for Spinal Cord Medicine. Preservation of upper limb function following spinal cord injury: A clinical practice guideline for health-care professionals. *Consortium for Spinal Cord Medicine: Clinical Practice Guidelines* . 2005.
36. AM Kwarciak, SA Sisto, M Yarossi, R Price, E Komaroff, and ML Boninger (2009): Redefining the manual wheelchair stroke cycle: identification and impact of nonpropulsive pushrim contact. *Arch Phys Med Rehab* 90:20.

37. I Rice, D Gagnon, J Gallagher, and M Boninger (2010): Hand rim wheelchair propulsion training using biomechanical real-time visual feedback based on motor learning theory principles. *J.Spinal Cord.Med.* 33:33.
38. AM Kwarciak, JT Turner, L Guo, and WM Richter (2010): Comparing handrim biomechanics for treadmill and overground wheelchair propulsion. *Spinal Cord.*
39. Jeffery Wade Rankin (2010): The Influence of Altering Wheelchair Propulsion Technique on Upper Extremity Demand. Unpublished dissertation. University of Texas at Austin.
40. AM Kwarciak, JT Turner, L Guo, and WM Richter (2012): The effects of four different stroke patterns on manual wheelchair propulsion and upper limb muscle strain. *Disability and Rehabilitation: Assistive Technology.* 22295946